

An approach for the identification of exemplar sites for scaling up targeted field observations of benthic biogeochemistry in heterogeneous environments

Thompson, Charlotte ; Silburn, Briony; Williams, Megan ; Hull, Tom; Sivy, David; Amoudry, Laurent; Widdicombe, Steve; Ingels, Jeroen ; Carnovale, Giorgia; McNeill, Caroline ; Hale, Rachel; Marchais, Claire Laguionie ; Hicks, Natalie ; Smith, Helen ; Klar, Jessie ; Hiddink, Jan; Kowalik, Jonathan; Kitidis, Vas ; Reynolds, Sarah ; Woodward, Malcolm ; Tait, Karen ; Homoky, William ; Kroger, Silke; Bolam, Stefan; Godbold, Jasmin; Aldridge, J.; Mayor, Dan; Benoist, Noelle ; Bett, Brian ; Morris, Kirsty ; Parker, Ruth; Ruhl, Henry; Statham, Peter; Solan, Martin

Biogeochemistry

DOI:

[10.1007/s10533-017-0366-1](https://doi.org/10.1007/s10533-017-0366-1)

Published: 01/09/2017

Peer reviewed version

[Cyswllt i'r cyhoeddiad / Link to publication](#)

Dyfyniad o'r fersiwn a gyhoeddwyd / Citation for published version (APA):

Thompson, C., Silburn, B., Williams, M., Hull, T., Sivy, D., Amoudry, L., Widdicombe, S., Ingels, J., Carnovale, G., McNeill, C., Hale, R., Marchais, C. L., Hicks, N., Smith, H., Klar, J., Hiddink, J., Kowalik, J., Kitidis, V., Reynolds, S., ... Solan, M. (2017). An approach for the identification of exemplar sites for scaling up targeted field observations of benthic biogeochemistry in heterogeneous environments. *Biogeochemistry*, 135(1-2), 1-34. <https://doi.org/10.1007/s10533-017-0366-1>

Hawliau Cyffredinol / General rights

Copyright and moral rights for the publications made accessible in the public portal are retained by the authors and/or other copyright owners and it is a condition of accessing publications that users recognise and abide by the legal requirements associated with these rights.

- Users may download and print one copy of any publication from the public portal for the purpose of private study or research.
- You may not further distribute the material or use it for any profit-making activity or commercial gain
- You may freely distribute the URL identifying the publication in the public portal ?

Take down policy

If you believe that this document breaches copyright please contact us providing details, and we will remove access to the work immediately and investigate your claim.

[Click here to view linked References](#)

1 An approach for the identification of exemplar sites for scaling up targeted field
2 observations of benthic biogeochemistry in heterogeneous environments.

3
4 Thompson, C.E.L.^{1*}, Silburn, B.², Williams, M.E.³, Hull, T.², Sivy, D.², Amoudry, L.O.³,
5 Widdicombe, S.⁴, Ingels, J.⁴, Carnovale, G.⁴, McNeill, C.L.⁴, Hale, R.¹, Laguionie Marchais, C.⁵,
6 Hicks, N.⁶, Smith, H.⁵, Klar, J.K.¹, Hiddink, J.G.⁷, Kowalik, J.⁸, Kitidis, V.⁴, Reynolds, S.⁹, Woodward,
7 E.M.S.⁴, Tait, K.⁴, Homoky, W.B.¹⁰, Kröger, S.², Godbold, J.A.^{1,11}, Aldridge, J.², Mayor, D.J.⁵, Benoist,
8 N.M.A.¹, Bett, B.J.⁵, Morris, K.J.⁵, Parker E.R.², Ruhl, H.A.⁵, Statham, P.J.¹, and Solan, M.¹.

9

10 ¹Ocean and Earth Science, University of Southampton, National Oceanography Centre, Southampton, SO14 3ZH, United Kingdom.

11 ²Centre for Environment, Fisheries and Aquaculture Science, Pakefield Road, Lowestoft, NR33 0HT, UK.

12 ³National Oceanography Centre, 6 Brownlow St, Liverpool, L3 5DA, UK.

13 ⁴Plymouth Marine Laboratory, Prospect Place, The Hoe, Plymouth, PL1 3DH, UK.

14 ⁵National Oceanography Centre, University of Southampton Waterfront Campus, European Way, Southampton, SO14 3ZH, UK.

15 ⁶Scottish Association for Marine Science, Scottish Marine Institute, Oban, Argyll, PA37 1QA, UK.

16 ⁷School of Ocean Sciences, Bangor University, Menai Bridge, LL59 5AB, UK.

17 ⁸Navama – technology for nature. Landshuter Allee 8, 80637 München, DE.

18 ⁹School of Earth and Environmental Sciences, University of Portsmouth, Burnaby Road, Portsmouth, PO1 3QL, UK.

19 ¹⁰University of Oxford, Department of Earth Sciences, South Parks Road, Oxford, OX1 3AN, UK.

20 ¹¹Biological Sciences, University of Southampton, Life Sciences Building, Highfield, Southampton, SO17 1BJ, UK.

21 *Corresponding author. email: celt1@noc.soton.ac.uk, Phone: 02380596855, Fax: 02380593131

22

23 Abstract

24 Continental shelf sediments are globally important for biogeochemical activity. Quantification of
25 shelf-scale stocks and flows of carbon and nutrients requires the extrapolation of observations
26 made at limited points in space and time. The procedure for selecting exemplar sites to form the
27 basis of this up-scaling is discussed in relation to a UK-funded research programme investigating
28 biogeochemistry in shelf seas. A three-step selection process is proposed in which (1) a target area
29 representative of UK shelf sediment heterogeneity is selected, (2) the target area is assessed for
30 spatial heterogeneity in sediment and habitat type, bed and water column structure and
31 hydrodynamic forcing, and (3) study sites are selected within this target area encompassing the
32 range of spatial heterogeneity required to address key scientific questions regarding shelf scale
33 biogeochemistry, and minimise confounding variables. This led to the selection of four sites within

34 the Celtic Sea which are significantly different in terms of their sediment, bed structure, and
35 macrofaunal, meiofaunal and microbial community structures and diversity, but have minimal
36 variations in water depth, tidal and wave magnitudes and directions, temperature and salinity. They
37 form the basis of a research cruise programme of observation, sampling and experimentation
38 encompassing the spring bloom cycle. Typical variation in key biogeochemical, sediment, biological
39 and hydrodynamic parameters over a pre to post bloom period are presented, with a discussion of
40 anthropogenic influences in the region. This methodology ensures the best likelihood of site-specific
41 work being useful for up-scaling activities, increasing our understanding of benthic biogeochemistry
42 at the UK-shelf scale.

43 **Keywords:** Benthic Biogeochemistry; Continental Shelf Seas; Ecosystem Services; Blue Carbon;
44 Nutrient Cycling.

45

46 **Acknowledgements**

47 This work was conducted under Workpackage 2 of the Shelf Sea Biogeochemistry programme
48 (SSB WP2, NE/K001906/1; NE/K002015/1; NE/K001744/1; NE/K001914/1; NE/K00204X/1;
49 NE/K001809/1; NE/K002139/1; NE/K001639/1; NE/K001922/1, 2011-2017), with inputs from
50 Workpackages 1 and 3 (NE/K002058/1; NE/K001973/1), jointly funded by the Natural Environment
51 Research Council (NERC) and the Department for Environment, Food and Rural Affairs (Defra).
52 The views expressed are those of the author(s) and not necessarily those of NERC or Defra. J.
53 Ingels was supported by a Plymouth Marine Laboratory Postdoctoral Research Fellowship in
54 collaboration with University of Exeter and a Marie Curie Intra-European Fellowship within the 7th
55 European Commission Framework Programme (Grant Agreement FP7-PEOPLE-2011-IEF no.
56 00879). W.B. Homoky was supported by a NERC Fellowship (NE/K009532/1). We extend our
57 thanks to the crew and scientists aboard the RSS Discovery cruises DY008, DY018, DY021,
58 DY026, DY029, DY030, DY033 and DY034 and RV Cefas Endeavour cruises 22/14, 03/15 who
59 provided the essential support needed for the collection of the data presented. Thanks go to Cefas
60 and NOC for their support of the Lander and SmartBuoy deployments and maintenance, and NERC
61 Marine Autonomous and Robotic Systems (MARS) group for the use of the Autosub AUVs. S-AIS
62 data analysis was supported by WWF and ORBCOMM. M5 wave buoy data was obtained from the

63 Marine Institute and Irish Meteorological Service. MODIS data was kindly supplied by NERC Earth
64 Observation Data Acquisition and Analysis Service (NEODAAS). Initial sampling / site selection
65 approaches and historic hydrographic, sediment and biological information drew on a large number
66 of Defra funded monitoring and R&D programmes namely: ME3205 (Marine Ecosystem
67 Connections; E5301 (Seabed Integrity); ME3112 (Irish Sea Benthos); MF1231 (Integrated
68 Ecosystem Survey) and historical hydrography data from AE1214, AE1225, AE1021.
69

70 **Introduction**

71 Continental shelf sediments make up less than 9% of the global seafloor, and yet are responsible
72 for the majority of global benthic biogeochemical cycling of organic matter (Jørgensen, 1983).
73 Despite their importance, it is still unclear whether benthic sediments act as a source or sink of
74 nutrients and carbon over extensive regions of the shelf (Nedwell et al, 1993), and the processes
75 that lead to changes in the internal pool of dissolved and particulate nutrients and carbon are not
76 fully understood (Hansen & Kristensen, 1997; Kristensen & Kostka, 2005). There remain a number
77 of key questions that need to be addressed in order to determine the importance of the seafloor in
78 moderating biogeochemical cycling and carbon and nitrogen stocks, and to reduce the uncertainty
79 associated with predicting the responses of shelf sea systems to natural variability and
80 anthropogenic forcing, including climate change (Viollier et al., 2003; Gruber, 2011; Solan et al, In
81 Prep). These include: (1) What are the short term (seasonal to annual/interannual) stocks and flows
82 of carbon and nutrients across a gradient of cohesive to non-cohesive sediments? (2) What is the
83 role of shelf sea sediments in long term (decades to centuries) carbon storage? (3) What is the role
84 of macrofaunal invertebrates in mediating benthic biogeochemistry?, and (4) what influence do
85 natural & anthropogenic disturbances have on these processes? Addressing these questions allows
86 us to establish the generalities of how abiotic and biotic interactions, including feedbacks and
87 linkages, will affect carbon and macronutrient exchange in shelf sea systems, and how they are
88 likely to change in the future.

89 A mismatch between measurements and models made across different temporal and spatial scales
90 limits our understanding of the biogeochemical processes that operate at the shelf scale (Capet et
91 al, 2016). As it is not technically possible to measure many variables at the scale of the shelf
92 system, detailed studies of representative shelf environments that span the full variety of
93 biogeochemical conditions offer an opportunity to gain mechanistic insights important for the
94 validation of modelling efforts (Savchuk, 2002). These field studies are often logistically challenging,
95 resulting in limited datasets relative to the intrinsic spatial and temporal variability of the shelf
96 (Cardoso et al., 2010). To allow successful scaling (of both resolution and extent) from these
97 studies to regional scales, interdisciplinary approaches which integrate both local- and macro-scale
98 data are most successful (Queiros et al, 2015; Painting et al., 2013). However, care must be taken

99 to identify the appropriate temporal and spatial scales whilst designing field programmes or when
100 interpreting collected data (Morrissey et al, 1992), as different scales can be important for different
101 variables (e.g. species richness vs. abundance: Archambault & Bourget, 1996; emergent behaviour
102 or lag periods: Godbold & Solan, 2013), and there may be critical scale thresholds for estimating
103 biogeochemical dynamics (Zhao & Liu 2014) and/or scale-dependent cascades of influence
104 between variables (e.g. Guichard & Bourget, 1998) that must be taken into account.

105 Given these considerations, shelf-wide studies must therefore combine in situ observations and
106 validation studies as well as manipulative laboratory and field experimentation to identify causal
107 relationships. These must all be integrated using a range of modeling approaches which simulate
108 spatio-temporal dependent changes in biogeochemical cycles and allow mapping of ecosystem
109 functioning and services (Edgar et al. 2016). A major challenge in achieving this goal is that
110 continental shelf seas exhibit high natural variability, both spatially (Mellianda et al, 2015; Stephens,
111 2015; Spinelli et al, 2004) and temporally (Reiss & Kröncke, 2005). They are highly spatially
112 heterogeneous in sediment coverage, with seafloor permeabilities ranging over seven orders of
113 magnitude (Spinelli et al, 2004), resulting in both diffusive and advective biogeochemical exchanges
114 occurring in close proximity. The end members (sand and mud) of these sediment types are
115 reasonably well defined (Precht & Huettel, 2003; Middelburg & Levin, 2009) but much less is known
116 about the intermediate mixed sediment types typical of the shelf. This spatial variability is mirrored in
117 the benthos where distinct meio- and macrofaunal assemblages are associated with changes in
118 sediment characteristics, water depth, and/or habitat heterogeneity over a wide range of scales
119 (LaFrance et al, 2014; Heip et al., 1985), although the mobility of these different communities
120 between closely spaced patches must also be considered (Levinton & Kelaher, 2004). In terms of
121 temporal variability, shelf sea water columns tend to be vertically mixed in the winter months, but
122 can become seasonally stratified during the summer due to heating and a reduction in wind and
123 wave-induced mixing (Simpson & Sharples, 2012). Stratification is often key to the initiation of the
124 spring bloom, and also has the potential to cause recurring periods of anoxia, associated with
125 changes in trace metals, nutrients and organic matter concentrations as well as benthic
126 communities (Stachowitsch, 2014). Modelling has shown significant variability in the timing of the

127 onset and breakdown of stratification (Young & Holt, 2007), with increasing air temperatures driving
128 a gradual trend to bring the spring bloom earlier (Sharples et al, 2006).

129 One problem, common in any representation of a complex environment (e.g. Zhang et al, 2004), is
130 that it is not possible to measure all of the key controlling parameters and processes essential to
131 regional assessments of biogeochemical cycling in all possible permutations of the varied benthic
132 habitats found on the shelf, and at all scales. It is paramount that any in situ measurements,
133 observation or experimentation are carried out at locations that represent appropriate exemplar
134 sites for the subsequent scaling up from point observations to the necessary regional predictions. It
135 has been suggested that the assessment of large numbers of small volume samples gives greater
136 precision than smaller numbers of larger samples (and is often more cost effective; e.g. Downing,
137 1989; Underwood, 1996), justifying a high-replication, small sample approach; but due to practical
138 limitations this necessitates a limited targeted area in which to work (reducing transit and therefore
139 sampling times).

140 For logistical reasons, one approach is to choose an area that contains suitable representative
141 habitat types within a constrained geographic region. The choice of area is based on a subset of
142 key controlling variables and ensures that sites are representative of typical conditions and cover
143 the range of heterogeneity found on the shelf, while variations in potential confounding variables
144 can be minimized.

145 It is likewise important to remember that continental shelves are also under significant pressure from
146 anthropogenic activities. Approximately 40% of the world's population lives within 100 km of the
147 coast, a density more than 3 times the global average (Cohen et al, 1997). Shelf seas provide
148 economic prosperity, as well as a range of essential services to these populations, including food
149 provision, recreation, waste disposal and increasingly energy production. Many of these uses
150 directly affect the benthic environment e.g. fishing using trawls, which accounts for 99.6% of the
151 spatial footprint of human activities on the seabed (Foden et al, 2010), impact upon the structure
152 and functioning of benthic communities (Kaiser et al, 1998; van Denderen, 2015), and the structure
153 and stability of the bed (Schwinghamer et al, 1998). It is not possible to remove the effects of these
154 pressures when investigating shelf-scale processes in situ, so careful consideration must be given

155 to these when findings are interpreted, including the differences between causative and correlated
156 relationships.

157 Here we present the approach adopted within the NERC and Defra-funded Shelf Seas
158 Biogeochemistry (SSB) programme to choose representative benthic sites on the UK continental
159 shelf. The overarching objectives of the SSB programme were to i) assess carbon and nutrients
160 cycling and their controls on primary and secondary production in UK and European shelf seas, ii)
161 to increase our understanding of these processes and their role in wider biogeochemical cycles, and
162 iii) significantly improve predictive marine biogeochemical and ecosystem models over a range of
163 scales. The approach taken is one of regional-local-regional scaling, which ensures a maintained
164 focus on the wider regional context throughout the project. Such nested sampling designs have
165 been shown to successfully overcome problems associated with spatial scaling (e.g. Morrissey et al,
166 1992), but are rarely applied at the outset of large multidisciplinary projects.

167

168 **Methodology**

169 The Celtic Sea covers an area of approximately 70,000 km² in the Atlantic Ocean to the west of the
170 UK. It exhibits the full range of sediment types typical of the UK shelf, with the additional benefit of
171 varied habitats found in close proximity, and the availability of previous and ongoing monitoring
172 activities in the region (e.g. Davis et al, 2014; Rippeth et al, 2014; Tweedle et al, 2013; Sharples et
173 al, 2013) and over a decade of ecosystem monitoring, research and development funded by the UK
174 government (see acknowledgements for details). It was therefore chosen as an area representative
175 of UK shelf sediment coverage as a whole ([Figure 1a](#)). Comparisons of benthic biodiversity around
176 the UK indicate similarities in infaunal assemblages on both the eastern and western UK shelves,
177 with observed variability dependant on tidal currents and sediment characteristics, and variability in
178 epifaunal assemblages also dependant on sediment type (Rees et al, 1998). This indicates that the
179 Celtic Sea is also a suitable proxy for UK shelf habitats (based on faunal communities; Connor et
180 al., 2004) if variations in sediment type (based on particle size; Folk and Ward, 1957) are taken into
181 account.

182 The site selection procedure involved a three step process in which a constrained target area within
183 the Celtic Sea was chosen, assessed for spatial and temporal heterogeneity, and finally, discrete
184 sites within this area were chosen as suitable for process studies.

185 **Sampling Techniques**

186 The Shelf Sea Biogeochemistry (SSB) Programme is an interdisciplinary programme, with wide
187 ranging objectives, aims and deliverables (<http://www.uk-ssb.org/>). As such, the full methodologies
188 for the techniques used to generate the data presented are referenced in the appropriate places
189 within the results section. However, the methods used to collect the samples during an 18 month
190 long cruise programme carried out between 2014 and 2015 are now described. All data collected
191 during the SSB programme is scheduled to be archived with the British Oceanographic Data
192 Centre, (<http://www.bodc.ac.uk>). Unless otherwise specified, statistical relationships between sites
193 are determined using the standard error of the mean, based on the central limit theorem.

194 **Water Column Observations and Sampling**

195 **Benthic Landers:** *Continuous Monitoring:* A series of benthic landers were designed by the Centre
196 for Environment, Fisheries and Aquaculture Science (Cefas) for continuous monitoring of near-bed
197 water column parameters. They were equipped with an ESM2 logger (Cefas, UK) measuring
198 conductivity and temperature (Aanderaa 3919B), pressure (Druck PDR 1828 20bar), turbidity
199 (Seapoint STM), oxygen saturation (Aanderaa Optode 3835) and chlorophyll fluorescence
200 (Seapoint SCF) for bursts of five minutes repeated every thirty minutes at a sampling frequency of 1
201 Hz. An upward facing RDI 600 kHz workhorse ADCP recorded in burst mode for five minutes every
202 hour at a sampling frequency of 1 Hz, which enabled hourly measurements of currents and
203 backscatter over approximately the bottom 40 metres of the water column, with the temporal
204 resolution to quantify turbulence. *Intra-tidal Monitoring:* The National Oceanography Centre (NOC)
205 Liverpool designed the miniSTABLE lander to allow shorter-term, higher frequency intra-tidal
206 monitoring of near-bed properties. This was equipped with a top mounted ADCP (RDI 1200 kHz),
207 bottom mounted Unisense oxygen eddy correlation system (Nortek Vector ADV, Unisense oxygen
208 microsensor, and Aanderaa oxygen optode), Aquascap Acoustic Backscatter Sensors (1,2,3,4 MHz),
209 3D ripple profiler (1.1 MHz dual axis pencil beam scanning sonar (Thorne and Hanes, 2002; Marine
210 Electronics, 2009)), Nortek Aqua-Dopp HR (2 Mhz) LISST-Holo, LISST 100X, McLane RAS water

sampling system, FSI CTD, and Satlantic SUNA nitrate sensor. **Buoys:** Cefas designed *SmartBuoys* provide a long term high-frequency time series (at 1 m below surface) of salinity, temperature, turbidity, oxygen saturation, chlorophyll fluorescence (sensors and sampling regime as for Continuous Monitoring Landers). A water sampler (Cefas Technology Ltd (CTL), UK) collected unfiltered samples, which were preserved for subsequent nutrient analysis. A quantum irradiance sensor (LiCor LI-192) mounted just above the sea surface provided long term measurements of the photosynthetically active light climate for the area. The *M5 Wexford Coast wave buoy* (51.69°N 06.704°W since 2004), part of the Irish Weather Buoy Network provided long-term wave parameters for the region. Lander and Buoy deployment locations and durations can be found in Online Resource 1. **Underway data:** Underway pCO₂ data were collected using the PML-Dartcom Live pCO₂ system during the cruise programme, sampling atmospheric pCO₂ and headspace equilibrated seawater pCO₂ every 20 minutes and calibrated against NOAA-traceable CO₂ standards with an accuracy of $\pm 4 \mu\text{atm}$ (Ribas-Ribas *et al.*, 2014). Underway chlorophyll *a* was determined fluorometrically and calibrated against known chlorophyll *a* standards (Welshmeyer, N. A., 1994). **CTD:** Water column profiles of temperature, salinity, depth, chlorophyll fluorescence and turbidity were collected, along with water samples for sensor calibration and nutrient analysis using both standard and titanium (ultra-clean) Sea-Bird CTD systems. Nutrient samples from the water column samples, and from benthic sediment profiles and experiments, were all analysed on board using a Bran and Luebbe segmented flow colorimetric autoanalyser following Woodward and Rees (2001). Clean sampling protocols were used to avoid contamination, and analysis and sampling were carried out as close as possible to international GO-SHIP protocols (Hydes *et al.*, 2010). Where the sample concentrations were high they were diluted with low nutrient seawater, to bring them within the analytical range of the analyser. Iron concentrations (both Fe(II) and total dissolved Fe) were determined spectrochemically by measuring the absorbance of the Fe(II)-ferrozine complex formed after the addition of ferrozine (and ascorbic acid for the determination of total Fe) to each sample (Stookey, 1970). Concentrations $> 1 \mu\text{M}$ were analysed in a 1 cm quartz cell on a spectrophotometer (ATI Unicam 8625) and concentrations $< 1 \mu\text{M}$ were measured on a 2.5 m 3000 Series Liquid Waveguide Capillary Cell (World Precision Instruments) (Waterbury *et al.*, 1997).

239 **Benthic Sampling**

240 **Autonomous Underwater Vehicle Survey:** The *Autonomous Underwater Vehicles (AUVs)*

241 Autosub3 and Autosub6000 (e.g. Morris et al, 2014) were used to survey the four chosen process
242 study sites. At each site the AUV surveyed between 3 and 6 transect lines 5 km in length, with a line
243 spacing of ~150 m, at a nominal speed of 1.4 m·s⁻¹. Data collected included: i) swath bathymetry
244 (50 m altitude) using a Kongsberg EM2000 multibeam system; (ii) sidescan sonar (15 m altitude)
245 using an EdgeTech 2200-FS; and (iii) photography (~3.2 m altitude) using a Point Grey Research,
246 Grasshopper2, mounted vertically downward. **Coring:** Principal sediment sampling was carried out
247 using a *NIOZ (Haja) Boxcorer (K16)* with 320 mm diameter cylindrical core barrels, providing a 0.08
248 m² core sample with overlying water. In many cases these were then sub-sampled to provide
249 specific sized cores or sediment samples for subsequent experimentation and analysis (described
250 in more detail below where necessary). Larger sediment samples for faunal analysis were collected
251 using an USNEL-type 500 mm square (0.25 m²) *Scottish Marine Biological Association (SMBA) Box*
252 *Corer*. A Bowers and Conelley *Megacorer* was used to take multiple (up to 12) simultaneous
253 sediment samples in 100 mm diameter pre-drilled polycarbonate core tubes up to 300 mm in length,
254 from an approximately 0.25 m² area of the seabed for iron analysis (Barnett et al., 1984; Aquilina,
255 2014; Homoky et al., 2013). **Trawls:** A Cefas 2 m *Jennings beam trawl* was used for the collection
256 of epifauna from 3 replicate 5 minute trawls carried out at ship speeds of 1.5 knots. The trawl is fully
257 described in (Jennings et al, 1999) and consists of a 60 mm square section beam with chain mat 2
258 m wide at the mouth, and a 20 mm mesh with a 4 mm knotless mesh liner. **Sediment Profile**

259 **Imaging:** A *Sediment Profile Imaging (SPI)* camera, manufactured by Ocean Imaging Systems, was
260 used to capture in-situ vertical profile images of the top few centimetres of the seabed, including the
261 sediment-water interface. This is a photographic technique (Rhoads & Cande, 1971; Germano et al,
262 2011) where a mirrored prism is driven vertically, by its own weight, into the sediment profile and
263 photographs intersecting the sediment-water interface are obtained 15 and 30 seconds after
264 penetration. It used a Nikon D100 digital camera (F10, 1/60th second, ISO400) with a 35 mm lens
265 and self-contained strobe flash unit.

266

Results

Step 1: Identifying a constrained target area within the Celtic Sea

Given the total area of the Celtic Sea, it was necessary to focus operations on a constrained area which is representative of the Celtic Sea, and the UK Shelf as a whole. The rationale for the selection of this broad target area was based on the identification of varied habitats typical of different sediment types (ranging from fine cohesive muds to coarse advective sands) that exhibit different biogeochemical exchange mechanisms; varied faunal abundance, diversity and function, while staying within a similar hydrodynamic environment. Confounding variables are reduced by adopting a narrow range of depth, temperature and hydrographic variations. To make this selection, a full assessment of the typical conditions within the Celtic Sea was necessary.

Regional Hydrodynamics

The Celtic Sea extends from the shelf-break at approximately 200 m depth, to a narrow, steep coastal zone. The inner shelf ([Figure 1b](#)) comprises depths between 70-120 m (Uncles & Stephens, 2007), and is generally featureless, with a more irregular outer shelf deeper than 120 m. Tides are predominantly semi-diurnal (e.g., Robinson, 1979), and the mean spring tidal range increases from approximately 3 m close to its South Western boundary near the shelf break to >12 m in the Upper Severn Estuary (Hydrographic Office, 1996). Spring tidal speeds are relatively low, typically 0.2 m s^{-1} close to the seaward boundary, but increasing to 1.6 m s^{-1} in the Bristol Channel (Uncles and Stephens, 2007). Tidal ellipses tend to be strongly elliptical with a clockwise rotation (e.g., Robinson, 1979), apart from a localised region of circular ellipses with anticlockwise rotation west of the Bristol Channel (Robinson, 1979; Brown et al., 2003; Simpson & Tinker, 2009). Tidal ellipses also become more rectilinear as you approach the English Channel. Bed shear stresses are typically $<0.5 \text{ Nm}^{-2}$ within the central regions ([Figure 2](#)) increasing towards the shallower English and Bristol Channels to the East and the Irish Sea to the North.

Winds are predominantly from the South West or West, and wave conditions change as the sea becomes shallower and more sheltered. Ten-year mean significant wave heights vary from 2 m (8 s peak wave period) near the shelf break to 1 m (6 s peak wave period) where the Celtic Sea meets the Irish Sea, while extreme values for a return period of 1 year reach significant wave heights in excess of 8 to 10 m and peak periods of approximately 15 s (Bricheno et al., 2015).

296 **Water Column Structure**

297 Mean winter bottom temperatures are typically 9-10 °C, increasing to 11-16 °C in summer (Uncles &
298 Stephens, 2007; Brown et al., 2003). Salinity exceeds 35 near the shelf edge, reducing slightly
299 toward the coast, and varies little seasonally. Winter mixing of the water column in the Celtic Sea
300 leads to a well mixed water column, which is reflected in a homogenous temperature profile
301 between surface and deeper waters. A weak thermocline develops in springtime which inhibits full
302 water column mixing, providing suitable conditions to initiate a spring bloom (Simpson & Sharples,
303 2012).

304 Spring blooms in the region are typically dominated by diatoms, which account for up to 80% of
305 primary production during this period (Joint et al., 1986). During the summer months, surface waters
306 become nutrient poor and therefore lacking in phytoplankton. However, the development of a
307 summer deep chlorophyll maximum positioned at the base of the thermocline in the vicinity of the
308 nutricline (Pingree et al., 1977; Hickman et al., 2009) is a well-known phenomenon. Smaller-celled
309 phytoplankton tend to dominate here due to competition for nutrients and include prymnesiophytes,
310 pelagophytes and the cyanobacteria *Synechococcus* (Hickman et al., 2009).

311 **Sediment Coverage**

312 The wider Celtic Sea area contains sediment types ranging from pure muds to gravels ([Figure 1](#)):
313 sediments typical of a shelf-sea environment (bedrock is excluded from the sediment coverage
314 model presented [Stephens & Diesing, 2015], however this has little impact on the project as it's
315 contribution to biogeochemical cycling is minimal in the UK shelf setting). To ensure a narrow range
316 of depth, temperature and hydrographic variations, a contiguous target area within the inner shelf
317 region of the Celtic Sea was selected with minimal bathymetric variation ([Figure 3b](#)), high
318 hydrodynamic and water column similarity, but which also encompassed the widest possible range
319 of seabed types ([Figure 3a](#)).

320 Within this selected target area, the sediments are dominated by muddy sands, sand, and gravelly
321 sands (comprising 92% of total sediment coverage; [Table 1](#)), which typify the wider Celtic Sea
322 region (88% total sediment coverage). The average water depth across the target area was 95 m
323 below chart datum.

324 **Fishing Activity**

325 Large scale commercial fisheries expanded comparatively recently in the Celtic Sea, but have had a
326 relatively large and consistent impact on the area (Blanchard et al, 2005). Fishing activities tend to
327 focus on specific areas (Sharples et al, 2013), targeting the Celtic Deep, shelf edge, and to a lesser
328 extent the central Celtic Sea region (Figure 4), where trawlers target the Norway lobster *Nephrops*
329 *norvegicus* on muddy grounds. Fishing occurs year-round at the Celtic Deep (with a slight reduction
330 in Jan-March), although a seasonal pattern is seen in more central regions, with the bulk of activities
331 taking place in spring and summer (Sharples et al, 2013). Vessel Monitoring System (VMS) data
332 from between 2009-2014 suggests a differing trend in fishing ground preferences within the Celtic
333 region when split by UK and non-UK vessels (Figure 4), likely driven by difference in gear
334 preference, target species, regulations, and fuel prices (Jennings et al, 2012).

335 **Step 1 Summary**

336 The selected target area provides a constrained region on the inner shelf of approximately 87 x 95
337 km (8265 km²) within which to limit long-term observational measurements, cruise operations and in
338 situ experimentation. This restricts sampling to an area of minimal topographic and depth variation,
339 away from the shallower coastal regions where bed stresses are higher, and increasingly varied,
340 and away from freshwater inputs which would affect salinity and temperature. The area contains a
341 wide range of sediment and therefore habitat types, and minimises variations in depth and regional
342 hydrodynamics. To further limit potential depth and hydrodynamic variations, an approximately 20
343 km wide transect running from the south-west to the north-east across this region (following the tidal
344 flow and predominant wave directions) was identified. The same selection conditions were met, but
345 the required coverage was reduced to an area of approximately 2500 km². The next step was then
346 to make a full assessment of the spatial heterogeneity within this new, limited, target area and
347 select discrete sampling sites suitable for repeat seasonal sampling, and representative of the
348 dominant habitat types and biogeochemical exchange mechanisms of the shelf.

349 **Step 2: Assessments of spatial and temporal heterogeneity within the target area and** 350 **implications for benthic habitats.**

351 The main observational and experimental work for the Shelf Seas Biogeochemistry programme was
352 carried out during 2014-2015. At the start of this cruise programme, a series of benthic landers and

SmartBuoys were deployed within the target area to measure long-term hydrodynamic conditions during the survey period ([Figure 5](#); Online Resource 1). Four benthic Landers were deployed at The Celtic Deep 2 (CD2L) and East of the Celtic Deep (ECD) both to the North of the region, Nymph Bank (NB) in the central region and East of Haig Fras (EHF) to the South. A SmartBuoy has been located at the Celtic Deep (CD) site since 2009, but was moved to Celtic Deep 2 (CD2) in 2012. In addition, a SmartBuoy was located at the shelf edge (Candyfloss) for assessments of shelf exchanges and links to the pelagic component of the SSB programme (http://www.uk-ssb.org/science_components/work_package_1/).

Regional Hydrodynamics

Measured tides in the target area (Figure 6) were dominated by the M2 tidal constituent, followed by S2 and N2 constituents resulting in semi-diurnal tides with significant spring-neap variations (Robinson, 1979). Total spring and neap amplitudes reached 3.1 m and 1 m respectively at CD2L (Figure 6a), reduced in the south to 2.9 m springs at EHF, and increased to the east to 3.4 m springs at ECD consistent with the wider shelf area. Measured near-bed currents are also summarised in Figure 6.2. While there is little difference in the lowpass current magnitude, the maximum spring currents are strongest at EHF (mean maximum spring current approximately 0.4 m s^{-1}), followed by CD2L and ECD (0.36 m s^{-1}) and weakest at NB (0.32 m s^{-1}). There is a similar behaviour for the maximum bed shear stress (mean spring maximum value of 0.60 Nm^{-2} at ECD, 0.48 Nm^{-2} at ECD and CD2L, and 0.37 Nm^{-2} at NB), but the minimum bed shear stress is significantly higher at ECD (0.02 Nm^{-2} versus zero at the other three locations) resulting in an increase of the mean bed shear stress. The tidal ellipses also vary from near circular ellipses at ECD to near rectilinear at EHF matching the expected behaviour for the wider Celtic Sea region, with the polarity of the ellipse anti-clockwise for ECD, CD2L and NB, but clockwise for EHF. Mean daily wind speeds between 2012 and 2015 were 8.1 m s^{-1} , with a maximum of 22.9 m s^{-1} . There is a strong seasonal signal, with daily mean values of 6.5 m s^{-1} during the summer, and 10.3 m s^{-1} in winter. The M5 Wexford coast wave buoy shows winter waves have a mean height of 2.3 m with a maximum recorded height of 8.1 m in January, and summer mean wave height of 1.4 m.

380 **Water Column Structure**

381 Measured surface temperatures since 2009 ranged between 8.06 - 19.73 °C (mean 13 °C).
382 Stratification formed in early April in both 2014 and 2015, with re-mixing in mid-December in 2014.
383 This is in keeping with prior observations (Brown et al, 2003). CTD data indicate that the mixed layer
384 depth was shallowest in August (~25 m), deepening from September. Surface temperatures during
385 the sampling period were typical of the overall temperature range in the Celtic Sea, with bottom
386 temperatures limited to ~12 °C ([Figure 7a](#)), reaching a maximum following re-mixing during the
387 winter months, and also closely following the trend for the wider Celtic Sea region. Salinity had a
388 narrow range between 34.8 and 35.3 as expected for this inner region of the shelf. Riverine input
389 from the southern coast of Ireland is relatively minor. Freshening during winter and spring is thus
390 primarily attributable to input from the River Severn (Brown et al, 2003). Profiles of PAR allow
391 calculation of vertical attenuation coefficients (K_d ; Kirk, 2003) between 0.1 and 0.25 m^{-1} in Summer
392 and Autumn, also typical of offshore shelf waters (Foden et al, 2008). Water clarity reaches higher
393 values in summer (ranging from 0.13 and 0.9 m^{-1}) and is limited in range in winter (0.2 and 0.4 m^{-1}).
394 The timing of the thermal stratification observed was supported by water column macronutrient
395 profiles collected from CTD deployments over the course of both pelagic and benthic SSB field
396 campaigns ([Figure 7b](#)). During winter months the water column is completely mixed with total
397 organic nitrogen (TOxN) concentrations between 6.3 - 6.8 μM at all water depths (March 2015).
398 Similarly, profiles of silicate (4.6 – 5.2 μM) and phosphate (0.56 – 0.77 μM) demonstrate the
399 homogeneity of the water column at that time. In early April 2015 the onset of stratification and
400 assimilation of nutrients is witnessed with surface concentrations of nitrate depleting to 4.9 μM while
401 bottom water concentrations increased to 7.4 μM . Silicate and phosphate followed suit but depletion
402 was not as pronounced, with surface concentrations at 4.3 μM and 0.4 μM , and bottom
403 concentrations at 5.1 and 0.6 μM respectively. By the end of April 2015 once the bloom had
404 successfully established, a strong nutricline is observed between 20 and 30 m. Here, nitrate
405 concentrations have been significantly depleted in surface waters to 0.01 μM , whilst bottom water
406 concentrations have increased further to 10.6 μM . Depletion of surface silicate (0.3 μM) and
407 phosphate (0.01 μM) is also witnessed with elevated concentrations of 5.7 μM and 0.8 μM
408 respectively, found at depth. These nutrient conditions are observed throughout the late

409 spring/summer period until the nitrate and phosphate surface water concentrations are further
410 depleted, falling below detection limits (Woodward & Rees, 2001). This highlights the biological
411 drawdown of nutrients from the surface waters and probable remineralisation of organic matter at
412 depth, combined with the absence of water column mixing during this period.

413 Data from SmartBuoys show that phytoplankton blooms are variable in both timing and magnitude
414 in the region, usually occurring in March or April. In 2011, peak Chlorophyll concentrations occurred
415 in March, reaching $16 \mu\text{g.L}^{-1}$. During the SSB survey period, maximum Chlorophyll peaks were more
416 modest ($3\text{--}4 \mu\text{g.L}^{-1}$) and occurred later in the season. Moderate Resolution Imaging
417 Spectroradiometer (MODIS; NASA) satellite data demonstrate that the spring bloom was initiated in
418 early April 2015 coinciding with the onset of stratification, with full bloom conditions observed by the
419 week of the 19th April 2015 ([Figure 7c](#)). The bloom lasted for approximately four weeks before
420 crashing by mid-May. During the summer months when surface waters were nutrient poor, the
421 phytoplankton population was reduced.

422 **Spatial sediment heterogeneity**

423 During March 2015, a broad-scale benthic survey was completed to assess the spatial
424 heterogeneity of the sediments within the previously defined target area (Figure 8). At each
425 sampling location NIOZ box cores were collected and subsampled for particle size, bulk sediment
426 characteristics, oxygen and pH profiles, pore-water nutrient concentration profiles and meio- and
427 macro- faunal assessment. SPI images were collected for visual determination of sediment type,
428 zone of mixing (previously the apparent redox potential discontinuity [aRPD]; Teal et al, 2010) and
429 bed roughness. SMBA cores were taken for measurements of megafaunal abundance and
430 assemblage.

431 The results of the survey will be reported in detail elsewhere (e.g. McCelland et al., in prep; Silburn
432 et al., in prep), and confirmed that the targeted area contained a range of sediment types from
433 sandy muds, through to gravelly sands, reflecting the wider shelf region (For full details, see Online
434 Resource 2). In summary, coarser sediments dominate the central region, and the percentage of
435 fine sediments (median grain size $<63 \mu\text{m}$), which ranges between 1.73 - 86.61% across the entire
436 area, increases towards the Northeast and Southwest corners ([Figure 8](#)). Multivariate statistical
437 analysis of particle size data suggested that the sites could be allocated to one of eight different

438 seabed types that corresponded well to the Folk and Ward (1957) textural group classifications for
439 sediment bed types. The majority of the samples (92%) were poorly to very-poorly sorted, fine to
440 very-fine skewed (80%) and mesokurtic to very leptokurtic (96%). When overlaid on the targeted
441 area it is clear that the sediment coverage map presented is successful at representing the range
442 and location of surface sediments in the Celtic Sea.

443 Faunal analysis of the spatial survey samples demonstrated that sediment particle size distributions
444 were generally a good predictor of macrobenthic community structure (McClelland et al., In Prep).
445 However, there was considerable overlap in community composition between closely related
446 sediment types. This was due principally to many benthic species present having broad habitat
447 preferences occurring in multiple sediment habitats. In addition, despite changes in community
448 composition between sediment types, levels of macrofaunal abundance, biomass and diversity
449 remained largely constant across all the samples with perhaps only a slight reduction in these
450 parameters for the sites with the highest fines percentages to the Northeast (McClelland et al.,
451 2016). Given that these sites were also subjected to the greatest intensity of trawling, this slight
452 reduction may be due more to anthropological disturbance than to any natural ecological process.

453 **Step 2 Summary**

454 The spatial survey demonstrated that the target area contained a wide range of benthic sediment
455 and habitat types typical of the wider Celtic Shelf region, while being exposed to minimal variations
456 in water depth, water column conditions and hydrodynamic forcings spatially, which all fall within the
457 ranges expected of the wider Celtic Sea area, but exhibit clear seasonal changes.

458 **Step 3a: Identify and describe exemplar sites for process studies which capture the** 459 **necessary range of benthic variability; Physical Conditions**

460 Final site selections were made based on the sediment maps and past cruise data presented
461 above, and were further refined using ground-truthing during the first SSB cruise in 2014 (Table 2),
462 and the spatial survey in 2015. Based on the sediment coverage data, four final process sites were
463 selected to fall within the targeted area, which would represent the overall range of habitat and
464 sediment types within the region, ranging across the end-member biogeochemical exchange
465 mechanisms (diffusive and advective). Discounting the gravel dominated sediments, due to the
466 practicalities of using the proposed experimental methods on gravels, there are four main sediment

types evident across the target area: mud; sandy mud; muddy sand and sand. Pure mud is of negligible coverage (0.005%) and so the sites chosen were a sandy mud (with as low a sand fraction as possible) to represent the diffusive end member, a sand sediment to represent the advective end member, and two muddy sand sites in between.

Each process site was represented by a 0.25 km² box (500 m x 500 m) within which sampling would be constrained, minimising local heterogeneity while ensuring sufficient space to resample the sites without on-going impacts from previous sampling efforts. Process site names represent the order in which they were ground-truthed and are presented according to decreasing fines percentage. The boxes with the highest percentages of fines (A) and sand (G) were used to represent the end-members of the observed spectrum, with the sites H and I displaying intermediate values on the continuum.

The full benthic Shelf Seas Biogeochemistry programme visited each site four times, to assess seasonal differences across each of the sites, and assess conditions prior to, during and after the spring bloom ([Table 2](#)).

These cruises used a combination of in situ observation, sediment and biological sampling and experimentation to make assessments of biogeochemical processes occurring at each of the sites. While site selection was based on data collected in DY008 and DY021, the data presented below represent typical values averaged over all four cruises, to provide baseline ranges throughout the year for each site, providing the most thorough assessment of site representativeness to the wider target area and Celtic Sea region.

Water Column Conditions

The long-term Lander data can be used to assess the hydrodynamic conditions occurring at the process sites ([Table 3](#)), to confirm whether the confounding variables were well constrained. The average water depth of the four sites was 106 m, and between site variation less than 10% of the total average water depth. This was confirmed by Autosub3 collected bathymetry data (Online Resource 3). Bottom temperatures over the sampling period averaged 9.76 °C, varying within 5% of this value between sites; salinity was 35.2 (<1% variation between sites). Significantly different spatial variations in turbidity (standard error of the mean; $p < 0.0001$) and O₂ saturation ($p < 0.0001$) were apparent, which given the water column similarities between the sites, likely result from

496 differences in the bed sediment or habitat type. Turbidity was the highest at ECD, which also
497 corresponded to the highest O₂ saturation. In general, there was a close correlation between these
498 two parameters.

499 Underway and Lander measured Chlorophyll concentrations indicate that the spring bloom occurred
500 concurrently across the sites, were in agreement with the MODIS satellite data for the Celtic Sea, in
501 2015, and closely correlated with the onset of stratification. The bloom resulted in similar
502 drawdowns of CO₂ ([Figure 9b](#)) at each site.

503 **Sediment Classification**

504 Sidescan surveys were undertaken as part of DY034 using Autosub3 ([Figure 10](#)). These
505 encompassed the immediate process sites (500 x 500 m black boxes), plus the surrounding areas.
506 High backscatter (light tones) likely represents area of coarser or more mixed sediments, whereas
507 low backscatter (dark tones) finer or more homogeneous sediments. The presence of bedforms at
508 Site G is clear, reducing in wavelength towards the north of the region (from ~130 m to ~25 m).
509 These also appear in the bathymetry data collected at site G (Online Resource 3). Presumed 'trawl
510 marks' are particularly evident at Site A, but also present at sites I and H.

511 SPI images ([Figure 11](#)) from the four process sites show clear visual differences in grain size,
512 surface roughness and sediment colour indicative of different sediment and habitat types.

513 Photographs from the Autosub3 survey were used to visually distinguish between habitat types and
514 divided into three broad categories: hard ([Figure 11a](#): > 50% of the photograph covered by cobbles
515 or boulders); intermediate ([Figure 11b](#): 1-49% coverage of granules, cobbles or boulders); and soft
516 ([Figure 11c](#): 100% coverage by sand or mud). Particle Size Analysis (PSA) of multiple sediment
517 samples taken from NIOZ box cores over the 4 cruises ([Table 4](#)) confirm that the differences
518 between mean values at each site are statistically significant.

519 The four sites exhibit statistically different averaged median grain sizes (standard error of the mean;
520 $p < 0.005$), although H and I fall into the same textural classification ([Table 4](#)). In summary: site A is
521 a very poorly sorted, very fine skewed, mesokurtic, very coarse silt, classified according to the Folk
522 classification scheme as a sandy mud; site I is a very poorly sorted, very fine skewed, leptokurtic
523 very fine sand, classified as a muddy sand; site H is a very poorly sorted, very fine skewed,

leptokurtic fine sand, also classified as a muddy sand; and, site G is a poorly sorted, fine-very fine skewed, very leptokurtic medium sand.

The structure of the near-bed sediment (top 5 cm) was also assessed for each of the sites ([Table 4](#)). Depth averaged dry bulk densities were statistically different between sites ($p < 0.005$), with the exception of H and I ($p = 0.48$). Porosity and permeability were significantly different in all cases ($p < 0.020$ and $p < 0.001$ respectively). As expected, bulk density and specific permeability both increase with median grain size, while porosity decreases.

Small-scale seabed topography was provided from acoustic images of the bed measured by the 3D Acoustic Ripple Profiler (ARP) on the miniSTABLE intra-tidal monitoring lander. Results for the four sites show a variation in bed height of up to 4 cm ([Figure 12](#)). Bed structures at the more cohesive sites (A, H and I) appear to be dominated by circular depressions, probably caused by benthic fauna. Ripples were observed at the sandy site with little if any migration in all cases. These ripples were predominantly two-dimensional in March and May with ripple height approximately 2-3 cm and ripple wavelength approximately 20-30 cm, and three-dimensional in August with height approximately 1 cm and wavelength approximately 15 cm. The footprint of the ARP is too small to capture the larger scale (~30 m) bedforms seen in the sidescan data.

Step 3a Summary

This analysis described confirms that the four process sites can be considered as statistically different from each other in terms of the sedimentary characteristics (a key scientific variable of the SSB programme), showing a clear and concurrently occurring seasonal signal (key variable), while being similar in terms of hydrodynamic parameters (confounding variables).

Step 3b: Identify and describe exemplar sites for process studies which capture the necessary range of benthic variability; Biological and Biogeochemical variables

Assessments were made of key biogeochemical and biological parameters ([Table 5](#), [Table 6](#)), measured over all four cruises, providing typical ranges found at each site.

Biogeochemical Parameters

Sediment total organic carbon and nitrogen content are both highest at site A, intermediate at H and I, and lowest at site G. These differences were significant (standard error of the mean; $p < 0.05$) in all cases, except organic nitrogen between H and G. Oxygen penetration depths are not

553 significantly different, with the exception of I and G, although total oxygen consumption was
554 significantly different between all sites except I and H. It should be noted however, that total oxygen
555 consumption ranges were calculated based on the combination of data from three different
556 analytical methods and are discussed in more detail in Hicks et al., (In Prep) and Smith et al., (In
557 Prep). Chlorophyll measured in the surface sediments at A was significantly higher than the other
558 three sites ($p < 0.001$), and significantly lower at G than at I ($p < 0.05$), although differences
559 between other sites were not significant. The zone of mixing, is significantly different at all sites ($p <$
560 0.05) being lowest at H, and highest at A. Surface roughness (measured from SPI images; e.g.
561 [Figure 11](#)) is similar at all the muddy sites, and only significantly different at G ($p < 0.05$), as
562 confirmed from the acoustic bed roughness measurements presented above (Figure 12).

563 **Pore Waters**

564 Samples of pore water nutrients were collected using a novel in situ device developed at Cefas and
565 described elsewhere (e.g. Duplisea et al., 2001; Trimmer et al., 2000; Trimmer et al., 2005;
566 Sciberras et al, 2016; Weston et al., 2008). Pore water nutrient concentrations were measured in
567 triplicate usually down to 20 cm using a depth variable resolution. Data for the top 10 cm are
568 presented ([Table 5](#)). The concentration of NH_4^+ ranged between 0.23 and 145 μM across all sites
569 and cruises. The concentrations at Sites A, H and I generally increased from the sediment surface
570 to 10 cm depth, and then tended towards asymptotic ([Figure 13](#)). At Site G, increases did not occur
571 until below 3-4cm depth. Silicate profiles showed similar trends as the NH_4^+ with higher
572 concentrations (3 to 368 μM).

573 TOxN was usually at a maximum in the top 2 cm except at Site G where values at depth were
574 occasionally higher than at the surface, with a maximum value of 16.6 μM . Nitrite ranged between
575 0.07 and 8.27 μM and was generally evenly distributed throughout the top 20 cm. The differences
576 between sites are not statistically significant, however, this is likely due in part to the large ranges
577 resulting from measurements averaged over the different seasons (e.g. [Figure 13a](#)). Ranges were
578 similar to those measured over the spatial survey ([Figure 13b](#)) and therefore considered
579 representative of the region as a whole, and the inherent variability in the profile shapes, likely due
580 to high variability in the vertical sediment structure, should be noted.

581 Porewater iron (Fe) was extracted at 1 – 2 cm depth intervals using Rhizon filters (0.15 μm), inserted
582 into pre-drilled holes in custom Megacorer tubes (Seeberg-Elverfeldt et al., 2005; Homoky et al.,
583 2013; Klar et al., In Prep). Typically, porewater Fe concentration maxima occurred in the shallow
584 subsurface (up to > 100 μM at approx. 5 cm depth) and decreased sharply across the oxic surface
585 layer (profiles not shown, see Klar et al., in prep). Average surface (0 to 2 cm depth) porewater Fe
586 concentrations were highest at site I, lowest at site H and intermediate at site A ([Table 5](#)). Most of
587 the porewater Fe was in its reduced and soluble Fe(II) form, and oxygen penetration depths exert a
588 strong influence on pore water Fe contents across the study sites (Klar et al., in prep).

589 **Diffusive Nutrient Fluxes**

590 Ten centimetre diameter sediment sub-cores were collected from the NIOZ cores and incubated
591 with overlying bottom water to assess diffusive fluxes of TOxN and nitrite, ammonia, silicate and
592 phosphate using two similar sampling methods (Trimmer, 1998; Mayor et al., 2012; Main et al.,
593 2015). Sub-samples taken from the overlying water provided a time-series of nutrient exchange,
594 and data presented here are combined from up to 11 cores from each of the three SSB cruises that
595 took place in 2015 ([Table 5](#), Online Resource 5). Fluxes are stated with reference to the sediments
596 (i.e a negative result indicates removal from the water column overlying the sediment). Where there
597 was no measurable change in nutrient concentrations, the flux is quoted as zero. Data are not
598 corrected for water column controls.

599 On average, the fluxes of all macronutrients were positive, indicating a general release of
600 macronutrients from the sediments into the water column. However, both negative and positive
601 nutrient fluxes were measured at all sites, except for silicate fluxes at site A, which were consistently
602 positive (0.206–3.741 $\text{mmol m}^{-2} \text{d}^{-1}$). The range of fluxes measured at each site for all nutrients was
603 such that there was no significant difference when considered spatially between sites. Both nitrite
604 and TOxN fluxes were lowest on average at site A and increased through sites I and H, with the
605 highest average fluxes at site G. The greatest range in nitrite and TOxN fluxes were at site H (-
606 0.035 – 0.132 $\text{mmol m}^{-2} \text{d}^{-1}$ and -0.586 – 0.649 $\text{mmol m}^{-2} \text{d}^{-1}$ respectively). The fluxes of ammonium
607 were highly variable at all four sites, and site I was the only one to be negative overall with an
608 average flux -0.003 $\text{mmol m}^{-2} \text{d}^{-1}$. Sites G and H had the highest fluxes of ammonium (> 0.04
609 $\text{mmol.m}^{-2}.\text{d}^{-1}$) with the greatest range at site H. Silicate fluxes were on average highest at site A

(1.212 mmol m⁻² d⁻¹) almost double that of the other sites. Site H and I silicate fluxes were very similar with the lowest fluxes at site G (0.531 mmol m⁻² d⁻¹). Phosphate fluxes were highest at Site A, which had a negative flux (into the sediment) on average (-0.018 mmol m⁻² d⁻¹) and had the smallest range of fluxes compared to the other three sites.

Diffusive iron (Fe) fluxes were calculated from porewater concentration gradients across the oxic surface layer by combining a 1-dimensional steady state transport equation with the kinetics of Fe(II) oxidation following previous studies (Homoky et al., 2012; 2013) and is described in detail by Klar et al., (In Prep)(Table 5). Diffusive fluxes were positive at all sites ranging from 0.01 to 54.4 x10⁻³ mmol m⁻² d⁻¹. Averaged across the year, diffusive Fe fluxes were highest at site A (14.4 ±19.7 x10⁻³ mmol m⁻² d⁻¹), and 3-times lower at the site in our assessment with the coarser sediments, site H (2.70 ±5.54 x10⁻³ mmol m⁻² d⁻¹). However the range in Fe flux calculations was also greatest at site A, and equal to the range across all sites, while the range was smallest at site H. It is important to note that our assessment of diffusive Fe flux requires a simplification of benthic exchange processes. For example, the role of advection at these sites is not accounted for in the presented results, and yet it can serve to enhance the transport of Fe, especially from more permeable sites (Reynolds et al., In Prep).

Variability in biological abundance, biomass and diversity

Large mobile epifauna

A 2 m Jennings beam trawl was used at each of the 4 sites, on each of the 3 cruises during 2015 to collect and quantify the large epifaunal species. Some shallow burrowing infauna were also collected, but for clarity all fauna collected in the trawls will be termed as epifauna.

At all sites, epifaunal organisms were rather sparsely distributed ([Table 6](#)). Average abundance was highest at site G, although differences between sites were not statistically significant. Average blotted wet weight biomass values were lowest at sites I and H, slightly higher at the site G and highest of all at the site A, with significant pair-wise differences between all sites ($p < 0.01$) except between A and H or G. Diversity was highest at H, with site G being just a little less diverse. Sites A and I had the lowest epifaunal diversity.

Autosub3 seabed photographs were also analysed to estimate faunal density and biomass during DY034 (following the methodology of Morris et al 2014; see also Durden et al., 2015). At the time of

639 survey, near-bottom water column turbidity at Site A prevented the acquisition of useful seabed
640 photographs. All megabenthos and demersal fish were counted, measured and identified to the
641 lowest taxonomic level possible (Table 6; Example images can be found in Online Resource 6).
642 Linear measurements were made to estimate the biovolume of individual specimens and were
643 converted to wet mass assuming unit specific gravity (Morris et al., 2014; Durden et al., 2015). In
644 the case of colonial and encrusting organisms, these were measured as single entities. For
645 comparability with trawl-caught megabenthos biomass data, our estimates were scaled to a
646 sampling unit equivalent to a trawl catch data (500 m²). Three phyla dominated the three sites: 1)
647 Cnidaria was the most dominant at Site I and H and the third dominant at Site G; 2) Arthropoda was
648 the second dominant at all sites; and 3) Echinodermata was the dominant at Site G and the third
649 dominant at Site H and I.

650 **Mega-infauna (> 1cm)**

651 At each site five replicate SMBA boxcores were collected and the sediment sieved over a 1 cm
652 mesh. These samples revealed that all sites contained very few large infaunal species with no
653 single sample containing more than a couple of individuals. It was concluded that, due to their low
654 densities, large (> 1cm) infaunal organisms were not a substantial part of the benthic fauna in the
655 study area and that adequate sampling of the benthic fauna was provided by the Jennings trawl
656 (large epifauna) and the 0.08 m² NIOZ boxcorer (macrofauna).

657 **Macro-infauna (> 1mm)**

658 A 0.08m² NIOZ box corer was used to collect 5 replicate cores at each of the 4 sites, on each of the
659 4 cruises. These cores were sieved over a 1mm mesh and the macrofauna retained were identified,
660 counted and weighed.

661 Macrofaunal abundance was highest at sites I and H. Site A had slightly lower average abundance,
662 significantly lower than H and G ($p < 0.05$) whilst site (G) had less than 50% of the abundance of the
663 other three sites ($p < 0.0001$).

664 In direct contrast to abundance, wet weight biomass (g m⁻²) was considerably (2-3x) higher at site A
665 than it was at the other three sites. This would indicate that the average body size of macrofauna
666 was larger at site A than at the other three sites.

667 The average number of species per 0.08 m² core (a measure of α -diversity) was highest in the
668 intermediate sites H and I, with significantly lower diversity seen at sites A ($p < 0.001$) and G ($p <$
669 0.0001). However, the cores taken at site G were much more variable in terms of species
670 composition and this higher variability in species between replicate samples (β -diversity) meant that
671 the total number of species identified at site G was the same as site I and only a little less than site
672 H. Site A displayed relatively low diversity compared to the other sites.

673 Macrofauna abundance and biomass data were combined with published trait information
674 describing modes of sediment reworking and mobility (Queirós et al, 2013) to calculate the average
675 community bioturbation potential (BPc) for each of the sites following Solan et al (2004). Whilst BPc
676 is not a direct measure of the process of bioturbation it does provide a theoretical estimate of the
677 potential of a community to biologically mix the sediment. All of the 4 sites displayed notably low
678 levels of BPc (mean \pm standard deviation) with the highest values of bioturbation predicted for the
679 muddy site A (36.70 ± 22.53), followed by site H (30.31 ± 20.33) and site I (25.01 ± 17.70). The
680 lowest levels of predicted bioturbation were for site G (19.11 ± 13.14). However, the ranges were
681 large.

682 Measured macrofaunal bioturbation ([Figure 14](#)) and bioirrigation activity was very low across the
683 Celtic Sea shelf compared to other UK shelf areas (Dauwe et al, 1998; Teal et al, 2008), and similar
684 across all sediment types observed. The median ($f\text{-SPI}L_{\text{med}}$, typical short-term depth of mixing),
685 maximum ($f\text{-SPI}L_{\text{max}}$, maximum extent of mixing over the long-term) and mean ($f\text{-SPI}L_{\text{mean}}$, time
686 dependent indication of mixing) mixed depths of particle redistribution are presented in Table 6. In
687 addition, the maximum vertical deviation of the sediment-water interface (upper – lower limit =
688 surface boundary roughness, SBR) provided an indication of surficial activity. Bioturbation is heavily
689 influenced by the presence of mobile active species, such as *Nephrops norvegicus* and *Goneplax*
690 *rhomboides*. Bioturbation activity was observed to peak in May with sediment surface mixing
691 occurring to a depth of approximately 5 mm.

692 **Meiofauna**

693 At all sites and during all four cruises, meiofauna ($>63 \mu\text{m}$) was subsampled from the 0.08m² NIOZ
694 box in three 50 ml syringe cores (2.8 cm diameter, approx. 10 cm deep). These were pooled and
695 preserved in 10 % borax-buffered formaldehyde solution. Meiofauna was extracted using Ludox

696 density separation (Somerfield & Warwick, 1996). Ten percent of each sample was investigated
697 under a stereoscopic microscope, major meiofauna taxa (phyla) were identified (Higgins & Thiel,
698 1988) and nematodes were picked out and mounted on glass slides (Somerfield & Warwick, 1996).
699 For biomass measurements, nematode width and length were measured using a Leica DM3000
700 compound microscope and DFC450C camera using Leica imaging software, and converted into wet
701 weight biomass using Andrassy's formula (Andrassy, 1956) adjusted for the specific gravity of
702 marine nematodes (i.e. 1.13 g cm^{-3}) and 12.5% C/wet weight ratio (Heip et al., 1985). Data from the
703 first two cruises (DY008 and DY021) are presented here.

704 Meiofauna at site A was most abundant with average densities over $800 \times 10^3 \text{ ind m}^{-2}$ and maximum
705 values of $> 1200 \times 10^3 \text{ ind m}^{-2}$. Sites I, G and H were very similar in terms of meiofauna abundance,
706 with average values lying between 550 and $600 \times 10^3 \text{ ind m}^{-2}$, however the differences are significant
707 ($p < 0.05$). Muddy sediments are known to harbour greater densities of nematodes (Steyaert et al.,
708 1999), the dominant meiofauna phylum with 85.6% (65.3-97.6%) of total abundance, so the high
709 densities at site A are likely a reflection of sediment composition and related interstitial space (i.e.
710 greater porosity in muddy sediments at site A, Table 5) available to meiofaunal organisms. These
711 values lie within the range of densities commonly found in marine subtidal areas (Heip et al., 1985).
712 In terms of biomass (based on nematodes) site A and I are very similar (1.13 ± 0.35 and 1.14 ± 0.48
713 $\text{g wet weight m}^{-2}$, respectively; $p = 0.97$), and G and H are similar (0.68 ± 0.17 and 0.73 ± 0.39 g wet
714 weight m^{-2} , respectively; $p = 0.701$). As with abundance values, biomass values lie within the ranges
715 observed for European subtidal areas (Heip et al., 1985) with distinct differences between muddy
716 and sandy sediments. All pairwise comparisons between sites A, I and G, H resulted in significant
717 biomass differences ($p < 0.05$).

718 On the phyla level, multivariate meiofauna community structure data was significantly different
719 between sites and cruises ($p \leq 0.01$), and, like abundance and biomass, considerable similarity was
720 found for site pairs A and I ($p = 0.635$), and G and H ($p = 0.054$), whilst all other pairwise
721 comparisons showed significant differences ($p \leq 0.05$).

722 **Microbes**

723 At each site, sediment was sub-cored using either 30 mL (for direct microbial counts) or 50 mL (for
724 molecular analyses) syringe cores. Samples for direct microbial counts were sectioned (0 – 10; 10 –

25; 40 – 60; and 80 – 100 mm), immersed in a 2 % glutaraldehyde solution and frozen at –80 °C, whereas samples for molecular analyses were immediately frozen intact at -80 °C. Microbial abundance was enumerated using microscopy (Manini & Danovaro, 2006), and biomass estimated assuming an average of 14 fg carbon per microbial cell (Kallmeyer et al. 2012). To quantify the ratio of archaeal and bacterial 16S rRNA genes in each sediment sample, DNA was extracted using the MoBio Powersoil Total RNA Isolation Kit with the DNA Elution Accessory Kit (MoBio, Carlsbad, USA) from sectioned sediment (0 – 10; 40 – 60; and 80 – 100 mm). 16S rRNA gene abundances were quantified using the PCR primer pairs and methods published in Tait et al. (2015). Porosity (Table 4) was a major determinant of microbial biomass, with the highest measurements at site A and the lowest measurements at site G (Figure 15). Biomass decreased with sediment depth for all except site G.

Bacterial 16S rRNA genes dominate the total microbial assemblages within coastal sediments, with reports of only 2 % of 16S rRNA genes affiliated with archaea (DeLong, 1992). Our data suggest a higher abundance of archaea in shelf sediments, in all sediment types examined, with little evidence of differences in the ratio of archaeal:bacterial 16S rRNA genes with depth. At site A, 29.7 % (\pm 16.5) of 16S rRNA genes were archaeal, and at site I this figure was 35.8 % (\pm 15.9), 38.3 % (\pm 20.9) at site H and 22.2 % (\pm 14.2) at site G; the differences between sites are significant ($p < 0.05$).

Step 3b Summary

Habitat variations across the four sites echo the differences in sediment variation seen within the constrained target area, and confirmed that the process study sites represent significantly different habitats. These differences were also reflected in the bulk biogeochemical properties of the bed, although seasonal variability in pore water concentrations and nutrient fluxes were sufficient to mask spatial variability between the sites.

Discussion

We have described the way the four process study sites, which encompass the range of sediment and habitat variation seen in UK shelf seas, were identified within a constrained target area of the Celtic Sea, for investigation within the benthic component of the SSB programme. The sites differ significantly in terms of sediment, habitat type and bed structure, whereas differences in

754 confounding physicochemical variables were minimised and seasonal changes (e.g. the phenology
755 and magnitude of the spring bloom) occurred concurrently across the sites. This provided discrete,
756 exemplar process study sites across the appropriate range of bed types to represent the wider
757 region, for targeted field campaigns as part of the SSB programme.

758 Logistical limitations to in situ observations, sampling and experimentation are unavoidable, and
759 decisions must often be made early in the project planning stages regarding site selection. In shelf
760 sea environments, which are both spatially and temporally variable at a range of scales, this site
761 selection process becomes particularly important; especially where results are intended to be up-
762 scaled and used to represent or model systems at shelf or regional scales.

763 In these cases, as in the SSB Programme, the key to addressing such issues is to consider these
764 scaling necessities from the outset, and to assess regional scales and variability during the site
765 selection process (e.g. Painting et al, 2013; Savchuck, 2002). Thorough evaluation of the previously
766 available datasets is paramount to ensure that what are often limited resources can be put to best
767 use to address the scientific questions being asked.

768 It is apparent that neither observations nor models in isolation are sufficient for a regional
769 assessment of benthic biogeochemical cycling; observationalists and modellers working together
770 can improve process understanding and scaling processes (e.g. Steiner et al, 2016; Queiros et al,
771 2015). Some of the key points to consider during the site selection process are: the
772 representativeness of any data collected to the desired model outputs (Steiner et al, 2016); the
773 number of observations needed to address key uncertainties that affect existing parameterisations;
774 the identification of processes not currently considered (Steiner et al, 2016); and the benefits of
775 interdisciplinary/holistic approaches to parameterisation (Queiros et al, 2015).

776 The methodology presented here is therefore to first assess shelf-scale variability in order to step-
777 down in scale to the local and then site scales consistent with the scientific requirements and
778 technical restrictions of the project. This will allow a clear pathway forward for the subsequent
779 upscaling required for shelf scale assessments of biogeochemical cycling, in contrast to site
780 selection based on isolated bed or local variables alone.

781 **Site Selection Considerations.**

782 **Spatial Heterogeneity**

783 Three scales of heterogeneity were assessed within the site selection process: shelf-; local- and
784 site-scale. These were assessed using a combination of existing data and models (shelf scale -
785 Stephens, 2015; Stephens & Diesing, 2015); observation (local scale - spatial survey; landers and
786 buoys; Autosub); and replication (site scale). Limited resources typically preclude the assessment of
787 shelf-scale heterogeneity directly through observation and therefore necessitate the use of existing
788 data, e.g. the British Geological Service (BGS) surface sediment database (DigSBS250). The use of
789 extant data has inherent limitations, including: temporal differences in sample collection; variable
790 resolution; and methodological differences in data collection or analysis. Nevertheless, these data
791 present a reasonable representation of the variability of the shelf sediments, if not an exact map of
792 their current extent and location. In combination with scaling approaches such as Stephens and
793 Diesing (2015), this provides sufficient overview for the selection of a targeted region. At the local
794 scale, spatial surveys, such as the ones carried out here, can be used to ground truth existing
795 sediment maps, giving additional confidence in the data that will subsequently be used during the
796 up-scaling process. Such surveys can generate large numbers of samples, restricting the number of
797 stations that can be visited and limiting replication, so a balance between resolution and resources
798 is necessary. At the site-scale, variability can be at the scale of mm to dm and the range of
799 measurements and experimental techniques being made often target different scales (for example
800 O₂ profiling at the μm to mm scale versus in situ flume deployments at m² scales). To address this,
801 sufficient replication is required to determine the variability within the data, in order to interpret
802 whether any temporal/seasonal changes observed fall within the natural spatial variability of the
803 sites (Mouret et al, 2016)).

804 In terms of the SSB work considered here, this process allowed a relatively simple justification to be
805 made for the selection of the process sites. The targeted area was determined based on a balance
806 of maximum sediment heterogeneity and minimum confounding variable complexity. The
807 assessment of the spatial variation within the targeted area 1) justified the use of the surface
808 sediment coverage model (presented in figures 1, 4 and 8), 2) allowed an assessment of the

809 representativeness of the area in comparison with the shelf as a whole, and 3) provided baseline
810 values of this variability with which to make the final site selection.

811 **Assessments of Confounding Variables**

812 Throughout the selection process, it was essential to maintain a clear focus on the scientific
813 objectives of the programme, set out in the overarching aims of the SSB programme. However, the
814 shelf is a complicated system, and local environmental conditions such as bottom water
815 temperature, oxygen and nutrient concentrations and pelagic primary production inputs are all
816 known to affect biogeochemical cycling within shelf sediments (e.g. Soetaert, et al., 1996; Dollar et
817 al, 1991; Wijsman et al., 1999; Soetaert et al., 2000; Van Cappellen et al., 2002; Fulweiler et al.,
818 2008; Dale et al., 2011). Because the focus of the SSB work is on bed type, these local conditions
819 are considered confounding variables, which can be a particular problem when smaller-scale
820 variables are extrapolated (Morrissey et al, 1992). The focus was therefore to minimise any
821 differences in these variables between the sites, so as to simplify analysis, and avoid the risk of
822 masking the signals of interest. In our case, the hydrodynamic variables, timing and onset of
823 stratification, and the phenology and magnitude of the spring bloom (Chlorophyll and CO₂-
824 drawdown) were similar across sites, thereby minimising the impact of these confounding variables.

825 **Minimum Site and Visit Numbers**

826 Deciding upon the number of sites that will be visited and the frequency of those visits requires
827 careful consideration of, amongst other things, necessary replicability, the importance of spatial
828 versus seasonal variability, and the scope of observations; as well as restrictions on ship time,
829 manpower and available funds. The resulting selection must reduce the number of sites to what is
830 logistically achievable whilst maintaining the delivery of the required scientific outcomes of the
831 project. In the case of the SSB programme, the key importance of the spring bloom on the
832 biogeochemical processes (Zhang et al, 2015) dictated the temporal visitation requirements
833 (minimum of 3 visits: pre-, during- and post- bloom); while the variations in sediment type were the
834 key factor considered in terms of spatial requirements (see Step 3; and Assessments of
835 Confounding Variables). As a minimum, the end-member conditions for a given parameter within the
836 region must be investigated, ideally with information at intermediate sites to 'fill in the gaps'. Given
837 the range of sediments present in the Celtic Sea area, the chosen end members were sandy mud

(>50 % fines) and sand (<15 % fines). Two additional intermediary sites representing fines percentages of ~20 and 30 % were considered sufficient to provide an overview of the region, and represent a gradient between the end-members. This resulted in the minimum requirement of four sites, and twelve site visits over the lifetime of the programme. To illustrate the scale of this programme, it should be noted that each 'site visit' resulted in the collection of approximately 60 NIOZ cores; 5 SMBA cores; 3 Megacores, trawls, CTD casts, water column samples, buoy and lander maintenance and deployment, experimental deployments and autonomous surveys.

Considerations for Data interpretation.

It is important to consider the following when interpreting the data collected from these sites and shelf seas in general.

Sediment vs. Habitat Type.

While the terms are often used interchangeably, they are commonly closely related (LeFrance et al., 2014; Heip et al., 1985), and the faunal analysis performed herein shows that sediment size is generally a good predictor of macrobenthic community structure (McCelland et al., In Prep), it should be noted that considerable overlap occurs in species occurrence between closely related sediment types. Hence, habitat and sediment type, while closely correlated, are referred to separately here. While several species showed a strong site preference, there was considerable overlap of several species abundance at several of the sites. A full discussion of species abundance and site preference can be found in Online Resource 7.

Anthropogenic Influences

Marine observations and experiments often aim to investigate conditions relative to a defined baseline condition, to quantify change (Franco et al, 2015). The UK shelf seas are under the influence of significant present and historical anthropogenic pressures, which prevent a no-influence baseline being established, and it is often difficult to predict how these pressures may have or will change over time. Best practice is therefore to establish the historical influences that occurred before the study, monitor those that occur during it, and interpret the results with these in mind. The anthropogenic influences are varied, and we will not consider all of them here, however, the effect of trawling has the largest spatial impact directly on the seabed, and we briefly discuss this below.

866 **Trawling Pressures**

867 Commercial fishing is extensive in our chosen sampling region, and many fishing techniques have a
868 considerable impact on the bed. Accurate assessments of the amount of different fishing activities
869 and their intensities, and potential effects can be difficult. Nevertheless, estimates can be made
870 using AIS (Automatic Identification System), which was introduced by the International Maritime
871 Organisation (IMO) in the 1990s to improve maritime safety and avoid ship collisions (Natale et al.,
872 2015; McCauley et al., 2016). All vessel positions in an area of 2nm around the process study sites
873 were obtained from a satellite derived AIS dataset (S-AIS) for the period between March 2013 and
874 August 2015. This dataset contains vessel positions at intervals of ~15 minutes, and vessels fishing
875 at a speed of less than 8 knots should therefore leave at least two records within each area.

876 Fishing vessels, their main gear type, engine power and overall length were obtained by matching
877 their MMSI from the AIS data to the EU fleet register (<http://ec.europa.eu/fisheries/fleet/index.cfm>).
878 Only actively towed bottom fishing gears were considered in this analysis. The speed of vessels
879 was calculated from the distance and time between subsequent records, and fishing was assumed
880 to occur between 1.5 and 5 knots. Trawl tracks were reconstructed by connecting AIS records from
881 individual vessels where the record sampling interval was <20 minutes. The width of the trawl gear
882 was calculated from the engine power or vessel length using relationships given in Eigaard et al.
883 (2015). Trawling is also evident from Autosub sidescan imaging (Figure 10; Online Resource 4)
884 although a detailed quantification of potentially trawled seabed area from the sidescan images will
885 come at a later date.

886 Trawling was intense and frequent in box A ([Figure 16](#)), with only a minor fraction not trawled in the
887 period from March 2013 to August 2015. On average, the entire box was trawled 4.23 times over
888 this period. The main gear used was otter trawls. The doors of otter trawls (and clumps for otter twin
889 trawls) can penetrate the sediment to depths up to 35 cm (Eigaard et al, 2015), but the sweeps and
890 ground rope will not penetrate more than a few cm. Trawling was less intense in boxes G and H with
891 only half of the box being trawled, and virtually absent in box I, which is mirrored by the sidescan
892 survey data presented (Figure 10; Online Resource 4).

893 This is only part of the story however. In order to estimate whether benthic trawling had impacted
894 noticeably on the structure of macrofaunal communities we calculated the average AZTI Marine

895 Biotic Index (AMBI) for each of the four process sites. This index is derived from the relative
896 distribution of individuals across five ecological groups spanning a range of sensitivities to
897 disturbance (Borja et al. 2000). The index is designed to calculate values that fall along a continuum
898 from 0 (a community completely dominated by sensitive species and therefore undisturbed) and 7
899 (a completely azoic sediment). Our data indicated that despite the high frequency of trawling
900 identified at some of the sites, AMBI scores were generally low, with the highest average score of
901 2.25 (± 0.54) being recorded at site A as expected (Online Resource 8). For the other sites the AMBI
902 scores were all lower, and within similar ranges (site I, 1.01 ± 0.40 ; site H, 0.74 ± 0.29 ; site G, $1.12 \pm$
903 0.31). This would suggest that benthic trawling may have had only a minor impact on the structure
904 of the macrofauna at 3 of our sites, and only at site A was there evidence that the communities were
905 even slightly disturbed. Consequently, the relatively low levels of macrofaunal abundance, biomass,
906 biodiversity and bioturbatory function seen at all our sites must be driven by some other factor or
907 factors. For the meiofauna, there was no indication for trawling disturbance at the phylum level
908 given the high abundance at site A and the community similarity between A and I. We expect,
909 however, that the physical disturbance will be evident in nematode genera/species data since
910 previous studies have documented that physical stress, such as trawling, impacts nematode
911 diversity, function and community structure (Schratzberger et al, 2009; Schratzberger & Jennings,
912 2002).

913 Trawling in a region can have an additional indirect impact on long-term studies such as this one:
914 both the NB and ECD landers were lost during June 2014, likely through trawling activities. When
915 they were relocated in October 2014, a new site was chosen (CD2L) which gained protection from a
916 known long term monitoring position of which fishermen were aware.

917 **Future Pressures**

918 An additional consideration when interpreting the data collected in a programme such as this is that
919 data collection focusses on a limited window of time - in this case a little over a year. Spatial
920 patterns are likely to change over time, and the interactive effects of spatial and temporal changes
921 are likely to mean that each site evolves along a different trajectory (Morrisey et al, 1992). The SSB
922 programme design is sufficient to capture seasonal cycles, but not climatic ones. We must consider
923 that longer scale temporal changes would have an effect on any future scenario modelling or

924 prediction, and that we are not able to capture that in the field. Our approach is to determine where
925 the sampled 'year' fits against the typical conditions experienced on the shelf, and use experimental
926 and laboratory work to investigate this.

927

928 **Conclusions**

929 The Shelf Seas Biogeochemistry programme set out to assess the importance of the key variables
930 of sediment type and seasonality on carbon and nutrient cycling in UK shelf seas. As part of this
931 programme, exemplar sites for mechanistic and deterministic measurements of benthic
932 biogeochemical processes were identified on the basis of their potential to aid future up-scaling
933 activities to the shelf-scale. Our observations and activities will increase our broad-scale
934 understanding of benthic biogeochemical processes and improve our predictive shelf-scale
935 modelling capabilities.

936 The choice of our study sites was based on a three-step selection process in which the regional
937 context of the UK continental shelf was the main focus. Initially, a constrained target area within the
938 Celtic Sea was chosen to be representative of the sedimentary heterogeneity encountered across
939 the wider UK shelf. This also provided a focal region for long-term observations, cruise operations
940 and in situ experimentation. Secondly, a detailed assessment of the spatial and temporal
941 heterogeneity within this target area was made. Lastly, four process study sites were chosen within
942 this region which captured the necessary range of benthic variability needed to address the
943 scientific focus of the benthic component of the SSB programme.

944 Assessment of this procedure has led to the following recommendations:

945 Step One: The initial choice of a targeted region of operations must allow a careful balance between
946 resources and scientific requirements. Sufficient variability in the key scientific variables should be
947 ensured, as well as a reduction in the potential effects of any confounding variables, and
948 minimisation of the overall size of the operational area for logistical purposes.

949

950 Step Two: A full assessment of the variability within this target area allows:

951 a) Confirmation of sufficient spatial heterogeneity;

- b) Assessments of the targeted region within the context of the wider continental shelf (i.e. is the region representative?);
- c) Determination of whether existing, larger scale models and predictions of shelf-scale heterogeneity (used in step 1) are accurate; essential for subsequent up-scaling.

Step Three: The final choice of process study sites requires them to:

- a) Fully encompass the range of spatial heterogeneity occurring across the target area;
- b) Be sufficiently different in terms of the key scientific variables;
- c) Be sufficiently similar in terms of confounding variables;
- d) Be small enough to minimise within-site heterogeneity, which can then be addressed through sufficient replication;
- e) Have sufficient replication across scales to have sufficient statistical power to find hypothesised differences among metrics.
- f) Be large enough to reduce over-sampling during repeat, seasonal visits.

In relation to the SSB programme, following the above procedure has led to the selection of four exemplar process study sites that spanned the full range of variability exhibited on the UK shelf. These sites were significantly different in terms of their sediment and habitat type, yet were highly similar in terms of confounding variables e.g. hydrodynamic forcing, water depth, temperature, and salinity. We contend that the proposed site selection procedure ensures a very strong likelihood of site-specific work being useful for up-scaling activities and thus increasing our understanding of benthic biogeochemistry at the UK-shelf scale.

976 **References**

- 977 Andrassy, I. (1956) The determination of volume and weight of nematodes. *Acta Zoologica*
978 (Hungarian Academy of Science), 2: 1-1.
- 979 Archambault, P. and Bourget, E. (1996). Scales of coastal heterogeneity and benthic intertidal
980 species richness, diversity and abundance. *Marine Ecology Progress Series*, 136: 111-121.
- 981 Astrium, (2015). Creation of a high resolution digital elevation model (DEM) of the British Isles
982 continental shelf. Final report to Defra, London.
- 983 Aquilina, A., Homoky, W.B., Hawkes, J.A., Lyons, T.W. and Mills, R.A. (2014). Hydrothermal
984 sediments are a source of water column Fe and Mn in the Bransfield Strait, Antarctica. *Geochimica*
985 *et Cosmochimica Acta*, 137: 64-80.
- 986 Barnett, P. R.O., Watson, J. and Connelly, D. (1984). A multiple corer for taking virtually undisturbed
987 samples from shelf, bathyal and abyssal sediments *Oceanologica Acta*, 7(4):399-408.
- 988 Blanchard, J.L. Dulvy, N.K., Jennings, S., Ellis, J.R., Pinnegar, J.K., Tidd, A. and Kell, L.T. (2005).
989 Do climate and fishing influence size-based indicators of Celtic Sea fish community structure?. *ICES*
990 *Journal of Marine Science: Journal du Conseil*, 62(3): 405-411.
- 991 Borja, A., Franco, J. and Pérez, V. (2000). A Marine Biotic Index to Establish the Ecological Quality
992 of Soft-Bottom Benthos Within European Estuarine and Coastal Environments. *Marine Pollution*
993 *Bulletin*, 40(12): 1100-1114.
- 994 Brown, J., Carrillo, L., Fernand, L., Horsburgh, K.J., Hill, A.E., Young, E.F. and Medler, K.J. (2003).
995 Observations of the physical structure and seasonal jet-like circulation of the Celtic Sea and St.
996 George's Channel of the Irish Sea. *Continental Shelf Research*, 23(6): 533-561.
- 997 Brown, J.M., Amoudry, L.O., Souza, A.J., and Plater, A.J. (2015). Residual circulation modelled at
998 national UK scale to identify sediment pathways to inform coastal evolution models, in: Wang, P.;
999 Rosati, J.D.; Cheng, J., (eds.) *The proceedings of the Coastal Sediments 2015*. Singapore, World
1000 Scientific.
- 1001 Bricheno, L.M., Wolf, J., Aldridge, J. (2015). Distribution of natural disturbance due to wave and tidal
1002 bed currents around the UK. *Continental Shelf Research*, 109: 67–77. doi:
1003 10.1016/j.csr.2015.09.013 .

1004 Cai, W.-J. and Sayles, F.L. (1996). Oxygen penetration depths and fluxes in marine sediments.
1005 Marine Chemistry, 52(2): 123-131.

1006 Capet, A., Meysman, F.J.R., Akoumianaki, I., Soetaert, K. and Grégoire, M. (2016). Integrating
1007 sediment biogeochemistry into 3D oceanic models: A study of benthic-pelagic coupling in the Black
1008 Sea. *Ocean Modelling*, 101: 83-100.

1009 Cardoso, A., Cochrane, S., Doemer, H., Ferreira, J., Galgani, F., Hagebro, C., Hanke, G.,
1010 Hoepffner, N., Keizer, P., Law, R., Olenin, S., Piet, G., Rice, J., Rogers, S., Swartenbroux, F.,
1011 Tasker, M. and Van de Bund. W. (2010). Scientific support to the European commission on the
1012 Marine strategy framework directive. 24336, Publications Office of the European Union,
1013 Luxembourg.

1014 Cohen, J.E., Small, C., Melinger, A., Gallup, J., Sachs, J., Vitousek, P.M. and Mooney, H.A. (1997).
1015 Estimates of coastal populations. *Science*, 278: 1209.

1016 Connor, D.W., Allen, J.H.,Golding, N.,Howell, K.L., Lieberknecht, L.M., Northen, K.O. and Reker,
1017 J.B. (2004). The Marine Habitat Classification for Britain and Ireland Version 04.05. In: JNCC (2015)
1018 The Marine Habitat Classification for Britain and Ireland Version 15.03. Accessed: 09/2016.
1019 jncc.defra.gov.uk/MarineHabitatClassification

1020 Dale, A.W., Sommer, S., Bohlen, L., Treude, T., Bertics, V.J., Bange, H., Pfannkuche, O., Schorp,
1021 T., Mattsdotter, M. and Wallmann. K. (2011). Rates and regulation of nitrogen cycling in seasonally
1022 hypoxic sediments during winter (Boknis Eck, SW Baltic Sea): Sensitivity to environmental
1023 variables. *Estuar. Coast. Shelf S.*, 95(1): 14–28.

1024 Dauwe, B, Herman, P.M.J., and Heip, C.H.R. (1998). Community structure and bioturbation
1025 potential of macrofauna at four North Sea stations with contrasting food supply. *Marine Ecology*
1026 *Progress Series*, 173: 67–83.

1027 Davis, C.E., Mahaffey, C., Wolff, G.A., and Sharples, J. (2014). A storm in a shelf sea: Variation in
1028 phosphorus distribution and organic matter stoichiometry. *Geophysical Research Letters*, 41(23):
1029 8452-8459. doi:10.1002/2014GL061949.

1030 DeLong, E.F. (1992). Archaea in coastal marine environments. *Proceedings of the National*
1031 *Academy of Sciences*, 89: 5685-5689.

1032 Dollar, S.J., Smith, S.V., Vink, S.M., Obrebski, S. and Hollibaugh, J. (1991). Annual cycle of benthic
 1033 nutrient fluxes in Tomales Bay, California, and contribution of the benthos to total ecosystem
 1034 metabolism. *Mar. Ecol. Prog. Ser.*, 79: 115–125.

1035 Downing, J.A. (1989). Precision of the mean and design of benthos sampling programmes: caution
 1036 revised. *Marine Biology*, 103(2): 231-234.

1037 Duplisea, D.E., Jennings, S., Malcolm, S.J., Parker, R. and Sivyer, D.B. (2001). Modelling potential
 1038 impacts of bottom trawl fisheries on soft sediment biogeochemistry in the North Sea. *Geochemical*
 1039 *Transactions*, 1(14): 1-6.

1040 Durden, J., Bett, B., Schoening, T., Morris, K.J., Nattkemper, T. & Ruhl, H. (2016). Comparison of
 1041 image annotation data generated by multiple investigators for benthic ecology. *Mar Ecol Prog Ser*
 1042 552:61-70 doi:10.3354/meps11775.

1043 Edgar, G.J., Bates, A.E., Bird, T.J., Jones, A.H., Kininmonth, S., Stuart-Smith, R.D. and Webb, T.J.
 1044 (2016). New approaches to marine conservation through the scaling up of ecological data. *Annual*
 1045 *Review of Marine Science*, 8: 435-461.

1046 Eigaard, O.R., Bastardie, F., Breen, M., Dinesen, G.E., Hintzen, N.T., Laffargue, P., Mortensen,
 1047 L.O., Nielsen, J.R., Nilsson, H.C., O'Neill, F.G., Polet, H., Reid, D.G., Sala, A., Sköld, M., Smith, C.,
 1048 Sørensen, T.K., Tully, O., Zengin, M. and Rijnsdorp, A.D. (2015). Estimating seabed pressure from
 1049 demersal trawls, seines, and dredges based on gear design and dimensions. *ICES Journal of*
 1050 *Marine Science*. doi: 10.1093/icesjms/fsv099.

1051 Engelund, F. (1953). On the laminar and turbulent flow of ground water through homogeneous
 1052 sand. *Transaction, Danish Academy of Technical Sciences*, 3: 105 pp.

1053 Foden, J., Sivyer, D.B., Mills, D.K. and Devlin, M.J. (2008). Spatial and temporal distribution of
 1054 chromophoric dissolved organic matter (CDOM) fluorescence and its contribution to light attenuation
 1055 in UK waterbodies. *Estuarine Coastal And Shelf Science*, 79: 707-717.

1056 Foden, J., Rogers, S.I. & Jones, A.P. (2010). Human pressures on UK seabed habitats: a
 1057 cumulative impact assessment. *Marine Ecology Progress Series*, 428: 33-47.

1058 Folk, R.L. (1954). The distinction between grain size and mineral composition in sedimentary rocks.
 1059 *Journal of Geology*, 62: 344-359.

1060 Folk, R.L. and Ward, W.C. (1957). Brazos River bar: a study in the significance of grain size
 1061 parameters. *Journal of Sedimentary Petrology*, 27: 3–26.

1062 Franco, A., Quintionob, V. and Elliott, M. (2015). Benthic monitoring and sampling design and effort
 1063 to detect spatial changes: a case study using data from offshore wind farm sites. *Ecological Indices*,
 1064 57: 298-304.

1065 Fulweiler, R., Nixon, S. and Buckley, B. (2010). Spatial and temporal variability of benthic oxygen
 1066 demand and nutrient regeneration in an anthropogenically impacted New England estuary. *Est.*
 1067 *Coast.*, 33: 1377–1390.

1068 Germano, J.D., Rhoads, D.C., Valente, R.M., Carey, D.A. and Solan, M. (2011). The use of
 1069 sediment profile imaging (API) for environmental impact assessments and monitoring studies:
 1070 lessons learned from the past four decades. *Oceanography and Marine Biology: An Annual Review*,
 1071 49: 235-298.

1072 Glud, R.N. (2008). Oxygen dynamics of marine sediments. *Marine Biology Research*, 4: 243-289.
 1073 doi: 10.1080/17451000801888726.

1074 Godbold, J.A. and Solan, M. (2013). Long-term effects of warming and ocean acidification are
 1075 modified by seasonal variation in species responses and environmental conditions. *Philosophical*
 1076 *Transactions of the Royal Society, B*. 368: 20130186.

1077 Gruber, N. (2011). Warming up, turning sour, losing breath: ocean biogeochemistry under global
 1078 change. *Phil. Trans. R. Soc. A*, 369: 1980-1996.

1079 Guichard, F. and Bourget, E. (1998). Topographic heterogeneity, hydrodynamics, and benthic
 1080 community structure: a scale-dependent cascade. *Marine Ecology Progress Series*, 171: 59-70.

1081 Hansen, K. and Kristensen, E. (1997). Impact of macrofaunal recolonization on benthic metabolism
 1082 and nutrient fluxes in a shallow marine sediment previously overgrown with macroalgal mats.
 1083 *Estuarine Coastal And Shelf Science*, 45: 613-628.

1084 Heip, C., Vincx, M., Vranken, G., (1985). The Ecology of Marine Nematodes. *Oceanography and*
 1085 *Marine Biology* 23: 399-489.

1086 Hickman, A.E., Holligan, P.M., Moore, C.M. et al. (2009). Distribution and chromatic adaptation of
 1087 phytoplankton within a shelf sea thermocline. *Limnology and Oceanography*, 54(2): 525-536.

1088 Hicks, N., Ubbara, G., Silburn, B., Smith, H., Kroger, S., Parker, R., Sivyer, D., Kitidis, V., Stahl, H.
 1089 and Hatton, A. (2016) Oxygen dynamics in shelf seas sediments incorporating seasonal variability.
 1090 Biogeochemistry. Submitted.

1091 Higgins, R.P. and Thiel, H. (1988). Introduction to the study of Meiofauna. Smithsonian Institution
 1092 Press, London. 488 pp.

1093 HMSO. (1980). The determination of chlorophyll a in aquatic environments 1980. In: Methods for
 1094 the estimation of waters and associated materials. HMSO 1980, ISBN 0 11 751674 0.

1095 Homoky, W.B., Severmann, S., McManus, J., Berelson, W.M., Riedel, T.E., Mills, R.A. & P.J.,
 1096 Statham (2012) Dissolved oxygen and suspended particles regulate the benthic flux of iron from
 1097 continental margins. *Marine Chemistry* 134-135, 59-70

1098 Homoky, W.B., John, S.G., Conway, T. and Mills, R.A. (2013). Distinct iron isotopic signatures and
 1099 supply from marine sediment dissolution. *Nature Communications*, 4: doi: 10.1038/ncomms3143.

1100 Hydrographic Office. (1996). Co-tidal and Co-range lines: British Isles and Adjacent waters.
 1101 Admiralty Chart No. 5058, UK Hydrographic Office, Taunton, UK.

1102 Hydes, D.J., Aoyama, M., Aminot, A., Bakker, K., Becker, S., Coverly, S., Daniel, A., Dickson, A.G.,
 1103 Grosso, O., Kerouel, R., van Ooijen, J., Sato, K., Tanhua, T., Woodward, E.M.S. and Zhang, J.Z.
 1104 (2010). The GO-SHIP Repeat Hydrography Manual: a collection of expert reports and guidelines;
 1105 IOCCP report No.14, ICPO publication series No. 134, version 1.

1106 Jennings, S., Lee, J. and Hiddink, J.G. (2012). Assessing fishery footprints and trade-offs between
 1107 landings value, habitat sensitivity, and fishing impacts to inform marine spatial planning and an
 1108 ecosystem approach. *ICES Journal of Marine Science*, 69(6): 1053-1063.

1109 Joint, I., Owens, N.J.P. and Pomroy, A.J. (1986). Seasonal production of photosynthetic
 1110 pictoplankton and nanoplankton in the Celtic Sea. *Marine Ecology Progress Series*, 28(3): 251-258.

1111 Jørgensen, B.B. (1983). Processes at the sediment-water interface. In: *The Major Biogeochemical*
 1112 *Cycles and Their Interactions* (Eds. Bolin & Cook). SCOPE 21, Wiley, New York, pp. 477-509.

1113 Kaiser, M.J., Edwards, D.B., Armstrong, P.J., Radford, K., Lough, N.E.L., Flatt, R.P., and Jones,
 1114 H.D. (1998). Changes in megafaunal benthic communities in different habitats after trawling
 1115 disturbance. *ICES Journal of Marine Science*, 55: 353–361.

1116 Kallmeyer, J., Pockalny, R., Adhikari, R.R., Smith, D.C., and D'Hondt, S. (2012). Global distribution
 1117 of microbial abundance and biomass in subseafloor sediment. *Proceedings of the National*
 1118 *Academy of Sciences*, 109: 16213-16216.

1119 Kirk, J.T.O. (2003). The vertical attenuation of irradiance as a function of the optical properties of
 1120 the water. *Limnology and Oceanography*, 48(1), 9–17.

1121 Kirsten, W.J. (1979). Automatic methods for the simultaneous determination of carbon, hydrogen,
 1122 nitrogen, and sulfur, and for sulfur alone in organic and inorganic materials. *Analytical Chemistry*,
 1123 51: 1173-1179.

1124 Klar, J, Statham, P.J., Homoky, W.B., Woodward, E.M.S, Chever, F, Lichtschlag, A, Harris, E,
 1125 Silburn, B. (2016). The seasonal occurrence and stability of dissolved and soluble Fe(II) generated
 1126 in an oxic shelf environment, *Biogeochemistry*, Submitted.

1127 Kristensen, E. and Kostka, J.E. (2005). Macrofaunal burrows and irrigation in marine sediments:
 1128 microbial and biogeochemical interactions. In: *Interactions between macro- and microorganisms in*
 1129 *marine sediments* (Eds. Kristensen, E., Haese, R.R. and Kostka, J.E.) *Coastal Estuarine Stud.* 60:
 1130 125-157. Doi: 10.1029/CE606p0125.

1131 LaFrance, M., King, J., Oakley, B., and Pratt, S. (2014). A Comparison of Top-Down and Bottom-Up
 1132 Approaches to Benthic Habitat Mapping to Inform Offshore Wind Energy Development. *Continental*
 1133 *Shelf Research*, 83: 24-44.

1134 Lee, J., South, A.B. and Jennings, S. (2010). Developing reliable, repeatable, and accessible
 1135 methods to provide high-resolution estimates of fishing-effort distributions from vessel monitoring
 1136 systems (VMS) data. *ICES Journal of Marine Science*, 67(6): 1260-1271.

1137 Levinton, J. and Kelaher, B. 2004. Opposing organising forces of deposit-feeding marine
 1138 communities. *Journal of Experimental Marine Biology and Ecology*, 300: 65-82.

1139 Main, C.E., Ruhl, H.A., Jones, D.O.B., Yool, A., Thornton, B. and Mayor, D.J. (2015). Hydrocarbon
 1140 contamination affects deep-sea benthic oxygen uptake and microbial community composition. *Deep*
 1141 *Sea Research Part I: Oceanographic Research Papers*, 100:79-87.

1142 Manini, E. and Danovaro, R. (2006). Synoptic determination of living/dead and active/dormant
 1143 bacterial fractions in marine sediments. *FEMS microbiology ecology*, 55: 416-423.

1144 Mayor, D.J., Thornton, B., Hay, S., Zuur, A.F., Nicol, G.W., McWilliam, J.M. and Witte, U.F. (2012).
 1145 Resource quality affects carbon cycling in deep-sea sediments. *The ISME journal*, 6(9): 1740-1748.
 1146 Marine Electronics. (2009). User manual for the 3D Sand Ripple Profiling Logging Sonar, issue 1.1,
 1147 Marine Electronics Ltd., Vale, Channel Islands, UK.
 1148 Mason, C. E. (2011). NMBAQC's Best Practice Guidance. Particle Size Analysis (PSA) for
 1149 Supporting Biological Analysis. National Marine Biological AQC Coordinating Committee.
 1150 McCauley, D.J., Woods, P., Sullivan, B., Bergman, B., Jablonicky, C., Roan, A., Hirshfield, M.,
 1151 Boerder, K. and Worm, B. (2016). Ending hide and seek at sea. *Science*, 351: 1148-1150.
 1152 McCelland et al. (2016). In prep.
 1153 Mellianda, E., Huhn, K., Alfian, D., Bartholomae, A. and Kubicki, A. (2015). Variability of surface
 1154 sediment redistribution in the high-energy coastal shelf environment at German Bight, North Sea.
 1155 *Aquaculture, Aquarium, Conservation and Legislation - International Journal of the Bioflux Society*,
 1156 8: 667-678.
 1157 Middelburg, J.J. and Levin, L.A. (2009). Coastal hypoxia and sediment biogeochemistry.
 1158 *Biogeosciences*, 6:1273- 1293.
 1159 Morris, K., B. Bett, J. Durden, V. Huvenne, R. Milligan, D. Jones, S. McPhail, K. Robert, D. Bailey &
 1160 H. Ruhl, (2014). A new method for ecological surveying of the abyss using autonomous underwater
 1161 vehicle photography. *Limnology and Oceanography: Methods* 12: 795-809.
 1162 Morrissey, D.J., Howitt, L., Underwood, A.J. and Stark, J.S. (1992). Spatial variation in soft-sediment
 1163 benthos. *Marine ecology progress series*, 81: 197-204.
 1164 Mouret, A., Anschutz, P., Deflandre, B., Deborde, J., Canton, M., Poirier, D., Gremare, A. and
 1165 Howa, H. (2016). Spatial heterogeneity of benthic biogeochemistry in two contrasted marine
 1166 environments (Arcachon Bay and Bay of Biscay, SW France). *Estuarine, Coastal and Shelf*
 1167 *Science*, 179: 51-65.
 1168 Natale, F., Gibin, M., Alessandrini, A., Vespe, M. and Paulrudm A. (2015). Mapping fishing effort
 1169 through AIS data. *PLoS ONE*, 10(6): e0130746.
 1170 Nedwell, D.B., Parkes, R.J., Upton, A.C. and Assinder, D.J. (1993). Seasonal fluxes across the
 1171 sediment-water interface, and processes within sediments. *Phil T R Soc*, A343: 519-529.

1172 Painting, S.J., van der Molen, J., Parker, E.R., Coughlan, C., Birchenough, S., Bolam, S., Aldridge,
 1173 J.N., Forster, R.M and Greenwood, N. (2013). Development of indicators of ecosystem functioning
 1174 in a temperate shelf sea: a combined fieldwork and modelling approach. *Biogeochemistry*, 113(1):
 1175 237-257.

1176 Pingree, R.D., Maddock, L. and Butler, E.I. (1977). Influence of biological-activity and physical
 1177 stability in determining chemical distributions of inorganic-phosphate, silicate and nitrate. *Journal of*
 1178 *Marine biological Association of the United Kingdom*, 57(4): 1065-1073.

1179 Precht, E. and Huettel, M. (2003). Advective pore-water exchange driven by surface gravity waves
 1180 and its ecological implications. *Limnology & Oceanography*, 48:1674-1184.

1181 Queirós, A.M., Fernandes, J.A., Faulwetter, S., Nunes, J., Rastrick, S.P.S., Mieszkowska, N., Artioli,
 1182 Y., Yool, A., Calosi, P., Arvanitidis, C., Findlay, H.S., Barange, M., Cheung, W.W.L. and
 1183 Widdicombe, S. (2015). Scaling up experimental ocean acidification and warming research: from
 1184 individuals to the ecosystem. *Global change biology*, 21(1): 130-143.

1185 Queirós, A.M., Birchenough, S., Bremner, J., Godbold, J.A., Parker, E.R., Romero-Ramirez, A.,
 1186 Reiss, H., Solan, M., Somerfield, P.J., Van Colen, C., Van Hoey, G., and Widdicombe, S. (2013). A
 1187 bioturbation classification of European marine infaunal invertebrates. *Ecology & Evolution*, 3: 3958 -
 1188 3985.

1189 Rees, H.L., Pendle, M.A., Waldock, R., Limpenny, D.S. and Boyd, S.E. (1999). A comparison of
 1190 benthic biodiversity in the North Sea, English Channel, and Celtic Seas. *ICES Journal of Marine*
 1191 *Science*, 56: 228–246.

1192 Reiss, H. and Kröncke, I. (2005). Seasonal variability of benthic indices: And approach to test the
 1193 applicability of different indices for ecosystem quality assessment. *Marine Pollution Bulletin*, 50:
 1194 1490-1499.

1195 Reynolds, S.E., Klar, J., Kitidis, V., Homoky, W.B., Chapman-Greig, L., Panton, A., Thompson,
 1196 C.E.L., Woodward, E.M.S., Statham, P. J. and Fones. G. R. (2016). Seasonal biogeochemical
 1197 cycling of permeable sediments in a shelf sea environment. In Prep.

1198 Rhoads, D.C. and Cande, S. (1971). Sediment profile camera for in situ study of organism-sediment
 1199 relations. *Limnology and Oceanography*, 16(1), 110–114. <http://doi.org/10.4319/lo.1971.16.1.0110>.

1200 Ribas-Ribas, M. Rérolle, V.M.C., Bakker, D.C.E., Kitidis, V., Lee, G.A., Brown, I., Achterberg, E.P.,
 1201 Hardman-Mountford, N.J. and Tyrrell, T. (2014). Intercomparison of carbonate chemistry
 1202 measurements on a cruise in northwestern European shelf seas. *Biogeosciences* 11, 4339-4355,
 1203 doi:10.5194/bg-11-4339-2014.

1204 Rippeth, T.P. Lincoln, B. J., Kennedy, H.A., Palmer, M.R., Sharples, J. and Williams, C.A.J. (2014).
 1205 Impact of vertical mixing on sea surface pCO₂ in temperate seasonally stratified shelf seas. *Journal*
 1206 *of Geophysical Research: Oceans*, 119(6), 3868-3882. doi:10.1002/2014JC010089.

1207 Robinson, I.S. (1979). The tidal dynamics of the Irish and Celtic Seas, *Geophys. J. R. Astr. Soc.*, 56:
 1208 159-197.

1209 Savchuk, O.P. (2002). Nutrient biogeochemical cycles in the Gulf of Riga: scaling up field studies
 1210 with a mathematical model. *Journal of Marine Systems*, 32(4): 253-280.

1211 Sciberras, M., Parker, R., Powell, C., Robertson, C., Kröger, S., Bolam, S. et al. (2016). Impacts of
 1212 bottom fishing on the sediment infaunal community and biogeochemistry of cohesive and non-
 1213 cohesive sediments. *Limnology and Oceanography*, 10.1002/lno.10354.

1214 Schratzberger, M., Lampadariou, N., Somerfield, P., Vandepitte, L., Vanden Berghe, E. (2009). The
 1215 impact of seabed disturbance on nematode communities: linking field and laboratory observations.
 1216 *Marine Biology* 156 (4): 709-724.

1217 Schratzberger, M., Jennings, S. (2002). Impacts of chronic trawling disturbance on meiofaunal
 1218 communities. *Marine Biology* 141 (5): 991-1000.

1219 Schwinghamer, P., Gordon, D.C., Rowell, T.W., Prena, J., McKeown, D.L., Sonnichsen, G. and
 1220 Guigné, J.Y. (1998). Effects of Experimental Otter Trawling on Surficial Sediment Properties of a
 1221 Sandy-Bottom Ecosystem on the Grand Banks of Newfoundland. *Conservation Biology*, 12: 1215–
 1222 1222. doi: 10.1046/j.1523-1739.1998.0120061215.

1223 Seeberg-Elverfeldt, J., Schlüter, M., Feseker, T. and Kölling. M. (2005). Rhizon sampling of
 1224 porewaters near the sediment-water interface of aquatic systems. *Limnology and Oceanography:*
 1225 *Methods*, 3(8) :361-371.

1226 Sharples, J., Ellis, J.R., Nolan, G. and Scott, B.E. (2013). Fishing and the oceanography of a
 1227 stratified shelf sea. *Progress in Oceanography*, 117: 130-139. doi:10.1016/j.pocean.2013.06.014.

1228 Sharples, J., Ross, O.N., Scott, B.E., Greenstreet, S.P.R. and Fraser, H. (2006). Inter-annual
1229 variability in the timing of stratification and the spring bloom in the North-western North Sea.
1230 *Continental Shelf Research*, 26(6): 733-751. doi:10.1016/j.csr.2006.01.011.

1231 Silburn, B., Kröger, S., Parker, R., Sivyer, D., Hicks, N., Powell, C., Greenwood, N. and Johnson, M.
1232 (2016). Benthic pH gradients in a range of shelf sea sediments linked to sediment characteristics
1233 and seasonal variability.. *Biogeochemistry*, in prep.

1234 Simpson, J.H., and Tinker, J.P. (2009). A test of the influence of tidal stream polarity on the
1235 structure of turbulent dissipation. *Continental Shelf Research*, 29: 320-332.

1236 Simpson, J.H. and Sharples, J. (2012). Introduction to the physical and biological oceanography of
1237 shelf seas. Cambridge University Press.

1238 Smith H.E.K., Hicks, N.R., Sivyer, D.B., Kitidis, V., Tait, K. and Mayor, D.J. (2016). Seasonal and
1239 spatial variability of benthic biomass, oxygen consumption and nutrient fluxes in shelf sea
1240 sediments. *Biogeochemistry*, Submitted.

1241 Soetaert, K., Herman, P.M. and Middelburg, J.J. (1996). Dynamic response of deep-sea sediments
1242 to seasonal variations: a model. *Limnology and Oceanography*, 41(8): 1651–1668.

1243 Soetaert, K., Middelburg, J.J., Herman, P.M. and Buis. K. (2000). On the coupling of benthic and
1244 pelagic biogeochemical models. *Earth Sci. Rev.*, 51(1-4): 173–201.

1245 Solan, M., Fones, G., Godbold, J.A. et al. (2016). Priority challenges for understanding how multiple
1246 aspects of socio-ecological change influence the stocks and flows of macronutrients and carbon in
1247 shelf sea sediments. *Current Opinion In Environmental Sustainability*. In Prep.

1248

1249 Solan, M., Cardinale, B.J., Downing, A.L., Engelhardt, K.A.M., Ruesink, J.L., and Srivastava, D.S.
1250 (2004). Extinction and ecosystem function in the marine benthos. *Science*, 306:1177–1180.

1251 Solan, M., Wigham, B., Hudson, I., Kennedy, R., Coulon, C., Norling, K., Nilsson, H. and
1252 Rosenberg, R. (2004). In situ quantification of bioturbation using time-lapse fluorescent sediment
1253 profile imaging (f-SPI), luminophore tracers and model simulation. *Marine Ecology Series*, 271: 1-
1254 12.

1255 Somerfield, P. and Warwick, R. (1996). Meiofauna in marine pollution monitoring programmes: a
1256 laboratory manual. MAFF Directorate of Fisheries Research Technical Series, 71 pp.

1257 Spinelli, G.A., Giambalvo, E.R. and Fisher, A.T. (2004). Sediment permeability, distribution, and
 1258 influence on fluxes in oceanic basement. In: Hydrogeology of the Oceanic Lithosphere, (Eds. Davis,
 1259 E.E. and Elderfield, H.) CU Press.

1260 Stachowitsch, M. (2014). Coastal hypoxia and anoxia: a multi-tiered holistic approach.
 1261 Biogeosciences, 11: 2281–2285.

1262 Stephens, D. (2015). North Sea and UK shelf substrate composition predictions, with links to
 1263 GeoTIFFs. *Centre for Environment, Fisheries and Aquaculture Science*,
 1264 doi:10.1594/PANGAEA.845468.

1265 Stephens, D. and Diesing, M. (2015). Towards Quantitative Spatial Models of Seabed Sediment
 1266 Composition. PLoS ONE 10(11): e0142502. doi:10.1371/journal.pone.0142502.

1267 Steyaert, M., Gamer, N., van Gansbeke, D. and Vincx, M. Nematode communities from the North
 1268 Sea: environmental controls on species diversity and vertical distribution within the sediment.
 1269 Journal of the Marine Biological Association of the UK, 79(02): 253-264.

1270 Stookey, L.L. (1970). Ferrozine - a new spectrophotometric reagent for iron. Analytical Chemistry,
 1271 42 (7): 779-781.

1272 Tait, K., Stahl, H., Taylor, P., and Widdicombe, S. (2015). Rapid response of the active microbial
 1273 community to CO₂ exposure from a controlled sub-seabed CO₂ leak in Ardmucknish Bay (Oban,
 1274 Scotland). International Journal of Greenhouse Gas Control, 38: 171-181.

1275 Teal, L.R., Bulling, M.T., Parker, E.R. and Solan, M. (2008). Global patterns of bioturbation intensity
 1276 and mixed depth of marine soft sediments. Aquatic Biology, 2: 207-218.

1277 Teal, L.R., Parker, E.R. and Solan, M. (2010). Sediment mixed layer as a proxy for benthic
 1278 ecosystem process and function. Marine Ecology Progress Series, 414: 27-40.

1279 Tett, P. (1987). Plankton. In: Biological surveys of estuaries and coasts. Estuarine and brackish
 1280 water sciences association handbook (Eds. Baker, J.M and Wolff, W.J.). Cambridge University
 1281 Press, Cambridge, U.K. 280-341.

1282 Thorne, P.D. and Hanes, D.M. (2002). A review of acoustic measurement of small-scale sediment
 1283 processes. Continental Shelf Research, 22: 603-632.

1284 Trimmer, M., Petersen, J., Sivyer, D.B., Mills, C., young, E. and Parker, E.R. (2005). Impact of long-
 1285 term benthic trawl disturbance on sediment sorting and biogeochemistry in the southern North Sea.
 1286 Marine Ecology Progress Series, 298: 79-94.

1287 Trimmer, M., Nedwell, D.B., Sivyer, D.B. and Malcolm, S.J. (2000). Seasonal benthic organic matter
 1288 mineralisation measured by oxygen uptake and denitrification along an inner and outer transect of
 1289 the River Thames estuary U.K. Marine Ecology Progress Series, 197: 103-119.

1290 Trimmer, M., Nedwell, D.B., Sivyer, D.B. and Malcolm, S.J. (1998). Nitrogen fluxes through the
 1291 lower estuary of the river Great Ouse, England: the role of the bottom sediments. Marine Ecology
 1292 Progress Series, 163: 109-124.

1293 Tweddle, J.F., Sharples, J., Palmer, M.R., Davidson, K. and McNeill, S. (2013). Enhanced nutrient
 1294 fluxes at the shelf sea seasonal thermocline caused by stratified flow over a bank. Progress in
 1295 Oceanography, 117: 37-47. doi:10.1016/j.pocean.2013.06.018.

1296 Uncles, R.J. & Stephens, J.A. (2007). Sea 8 Technical Report - Hydrography. Strategic
 1297 Environmental Assessment Programme, UK Dept. of Trade and Industry, 105 pp.

1298 Underwood, A.J. 1996. Experiments in Ecology. Their logical design and interpretation using
 1299 analysis of variance. Cambridge University Press, 524pp.

1300 Van Cappellen, P., Dixit, S. and van Beusekom, J. (2002). Biogenic silica dissolution in the oceans:
 1301 reconciling experimental and field-based dissolution rates. Global Biogeochem. Cycles, 16(4): 23–1.

1302 van Denderen, P.D., Bolam, S.G., Hiddink, J.G., Jennings, S., Kenny, A., Rijnsdorp, A.D., & van
 1303 Kooten, T. (2015). Similar effects of bottom trawling and natural disturbance on composition and
 1304 function of benthic communities across habitats. Marine Ecology Progress Series, 541: 31-43. doi:
 1305 10.3354/meps11550.

1306 Viollier, E., Rabouille, C., Apitz, S.E., Breuer, E., Chaillou, G. and Dedieu, K. (2003). Benthic
 1307 biogeochemistry: state of the art technologies and guidelines for the future of in situ survey. Journal
 1308 of Experimental Marine Biology and Ecology, 285/286: 5–31.

1309 Waterbury, R.D., Wensheng Y. and R.H. Byrne. (1997). Long pathlength absorbance spectroscopy:
 1310 trace analysis of Fe(II) using a 4.5 m liquid core waveguide. Analytica Chimica Acta, 357(1–2): 99-
 1311 102.

1312 Welshmeyer, N. A. (1994). Fluorometric analysis of chlorophyll a in the presence of chlorophyll b
 1313 and phaeopigments. *Limnology and Oceanography* 39, 1985-1992.

1314 Weston, K., Fernand, L., Nicholls, J., Marca-Bell, A., Mills, D., Sivy, D. and Trimmer, M. (2008).
 1315 Sedimentary and water column processes in the Oyster Grounds: A potentially hypoxic region of the
 1316 North Sea. *Marine Environmental Research*, 65(3): 235-249.

1317 Wijsman, J.W., Herman, P.M. and Gomoiu. M.-T. (1999). Spatial distribution in sediment
 1318 characteristics and benthic activity on the northwestern Black Sea shelf. *Mar. Ecol. Prog. Ser.*, 181:
 1319 25–39.

1320 Woodward, E.M.S. and Rees, A.P. (2001). Nutrient distributions in an anticyclonic eddy in the North
 1321 East Atlantic Ocean, with reference to nanomolar ammonium concentrations. *Deep Sea Research*
 1322 II, 48(4-5): 775-794.

1323 Young, E.F. and Holt, J.T. (2007). Prediction and analysis of long-term variability of temperature and
 1324 salinity in the Irish Sea, *J. Geophys. Res.*, 112: C01008, doi:10.1029/2005JC003386.

1325 Zhang, X., Drake, N.A., and Wainwright, J. (2004). Scaling issues in environmental monitoring. In:
 1326 *Environmental Modelling: Finding simplicity in complexity* (Eds. Wainwright, J & Mulligan, M). Wiley.
 1327 69-90.

1328 Zhang, Q., Warwick, R.M., McNeill, C.L., Widdicombe, C.E., Sheehan, A. and Widdicombe, S.
 1329 (2015). An unusually large phytoplankton spring bloom drives rapid changes in benthic diversity and
 1330 ecosystem function. *Process in Oceanography*, 137(B): 533-545.

1331 Zhao, S and Liu, S. (2014). Scale critically in estimating ecosystem carbon dynamics. *Global*
 1332 *Change Biology*, 20(7): 2240-2251.

1333

1334 List of Figures

1335 **Fig 1** Spatial variations of (a) surface sediment type for the UK shelf (inset) and Celtic Sea areas
1336 using simplified Folk textural classifications, based on BGS surface sediment maps (Stephens,
1337 2015; Stephens and Diesing, 2015; Folk, 1954); and (b) Bathymetry, relative to Chart Datum based
1338 on 6 arcsec Defra Digital Elevation Map (Astrium, 2015)

1339 **Fig 2** Mean (a), minimum (b) and maximum (c) bed shear stresses (Nm^{-2}) typical of winter
1340 conditions within the Celtic Sea region. Stresses are obtained from a model simulation for a full year
1341 using ~ 1.8 km resolution for the entire northwest European shelf (Brown et al., 2015) where
1342 maximum tidal stresses that year occurred in October

1343 **Fig 3** Spatial variations of (a) surface sediment type using simplified Folk textural classifications,
1344 based on BGS surface sediment maps (Stephens, 2015; Stephens and Diesing, 2015; Folk, 1954);
1345 (b) Bathymetry relative to Chart Datum based on 6 arcsec Defra Digital Elevation Map for the
1346 chosen targeted area, overlaid with final sampling station positions. (Astrium, 2015)

1347 **Fig 4** Figure 4: Fishing Pressure in the Celtic Sea areas a) UK vessels and b) Non-UK vessels.
1348 VMS data held by the Marine and Fisheries Agency (MFA) of the UK Department of Environment,
1349 Food and Rural Affairs (DEFRA). Calculated effort as Hours times Engine Power per Year ($h \cdot \text{kw/y}$),
1350 based on aggregated VMS data of bottom trawled gears, vessel speed between 1-6 knots, from
1351 2009-2014. (normalised by year) with cell size 0.05 decimal degrees (Following the methods of Lee
1352 et al, 2010). Target area and process sites are identified

1353 **Fig 5** Lander and Smartbuoy positions within the targeted area (outlined in red). Locations of the
1354 final process study sites also identified. For deployment coordinates, see Online Resource 1

1355 **Fig 6** Tidal characteristics at: (1) Celtic Deep 2 Lander site. Showing (a) whole deployment
1356 elevation, (b) first month and (c) cumulative spectral density with main tidal components highlighted.
1357 (2) The four lander sites. Showing a) 25-hour running average of current speed at 2.9m above the
1358 bed b-e) Tidal ellipses for the four lander deployments, where U = East and V = North; colour
1359 scheme maintained between panels (2a) and (2b-e)

1360 **Fig 7** a) Daily mean temperatures: red represents surface temperatures measured by the Celtic
1361 Deep 2 SmartBuoy; cyan shows near bed temperature measured by the Cefas Continuous
1362 Monitoring Lander at Nymph Bank/Celtic Deep 2 Lander sites. b) Timeseries of nitrate and nitrite,

phosphate and silicate (mM) between March 2014 and August 2015 at Celtic Deep. c) MODIS Surface chlorophyll (mg L⁻¹) for the Celtic Sea, March – August 2015

Fig 8 Target area Particle Size Analysis of sediment samples 0-5cm depth analysed following the NMBAQC method (Mason, 2011) overlaid onto interpolated surface sediment map (Stephens, 2015; Stephens and Diesing, 2015; Folk, 1954)

Fig 9 (a) Chlorophyll fluorescence from 2014, indicating concurrent bloom timing. Rolling 24hr mean from Continuous Monitoring Lander. (b) Chlorophyll and sea-air CO₂ partial pressure gradient (DpCO₂) at stations A, H and G for 2015

Fig 10 Sidescan surveys of wider areas surrounding the final process site selections. (a) Site A, (b) Site G, (c) Site I and (d) Site H. Close up images from the sites themselves (black boxes) can be found in Online Resource 4)

Fig 11 (top) Sediment Profile Imagery (SPI) of the sediment-water interface and sub-surficial sediment profile at the 4 process sites. Image width 15 cm. (bottom) Autosub3 images of (a) hard; (b) intermediate and (c) soft sediment types

Fig 12 Acoustic images of relative bed roughness from the intra-tidal miniSTABLE Lander, August 2015

Fig 13 (a) Example pore water profiles with depth, Box I. (b) Example pore water silicate concentrations - main stations in triplicate (dark blue lines) overlaid on spatial survey stations (light blue)

Fig 14 Mean mixing depths across the process sites, associated with macrofaunal infaunal bioturbation: a) March 2014; b) March 2015; c) May 2015; d) August 2015

Fig 15 Microbial biomass (mm C m⁻²), estimated from direct counts of microbes. Station A = filled circles, station I = filled squares, station H = open triangle and station G = open diamond. Error bars are standard deviation

Fig 16 Trawl tracks across the four process study sites (500 x 500 km, represented by the black squares) between March 2013 and August 2015, indicating frequency and width of trawl tracks

List of Tables

1390 **Table 1** Percentage surface sediment coverage based on Folk Textural Classification categories for
 1391 the Celtic Sea area in Figure 1a and the target area in Figure 4a, highlighting those sediment types
 1392 which comprise >10% of the total (Stephens, 2015; Stephens & Diesing, 2015; Folk, 1954)

1393 **Table 2** Sampling and cruise periods, with central points of each 500m x 500m process site box

1394 **Table 3** Summary of continuous monitoring Lander data, presenting mean and standard deviation
 1395 of parameters for entire duration of deployment (min-max range in brackets)

1396 **Table 4** Sediment characterization and structural parameters for the four process study sites

1397 **Table 5** Biogeochemical Parameters

1398 **Table 6** Biological Parameters

1399 List of Online Resources

1400 **Online Resource 1** Long Term Observation deployment positions and operation timescales

1401 **Online Resource 2** Spatial survey sediment characteristics, organised by % Fines < 63µm

1402 **Online Resource 3** Bathymetric maps generated from Autosub3 (a) site A, (b) site G, (d) site I and
 1403 Autosub6000 (d) site H multibeam data (smoothed at 50 m horizontal scale). Water depth ranged
 1404 from 101-106 m at Site A, with the study box having a general depth of 103 m; 96-101 m at Site G,
 1405 study box general depth of 98 m; 106-107 m at site I, study box general depth of 107 m; 103-109 m
 1406 at Site H, study box general depth of 105 m

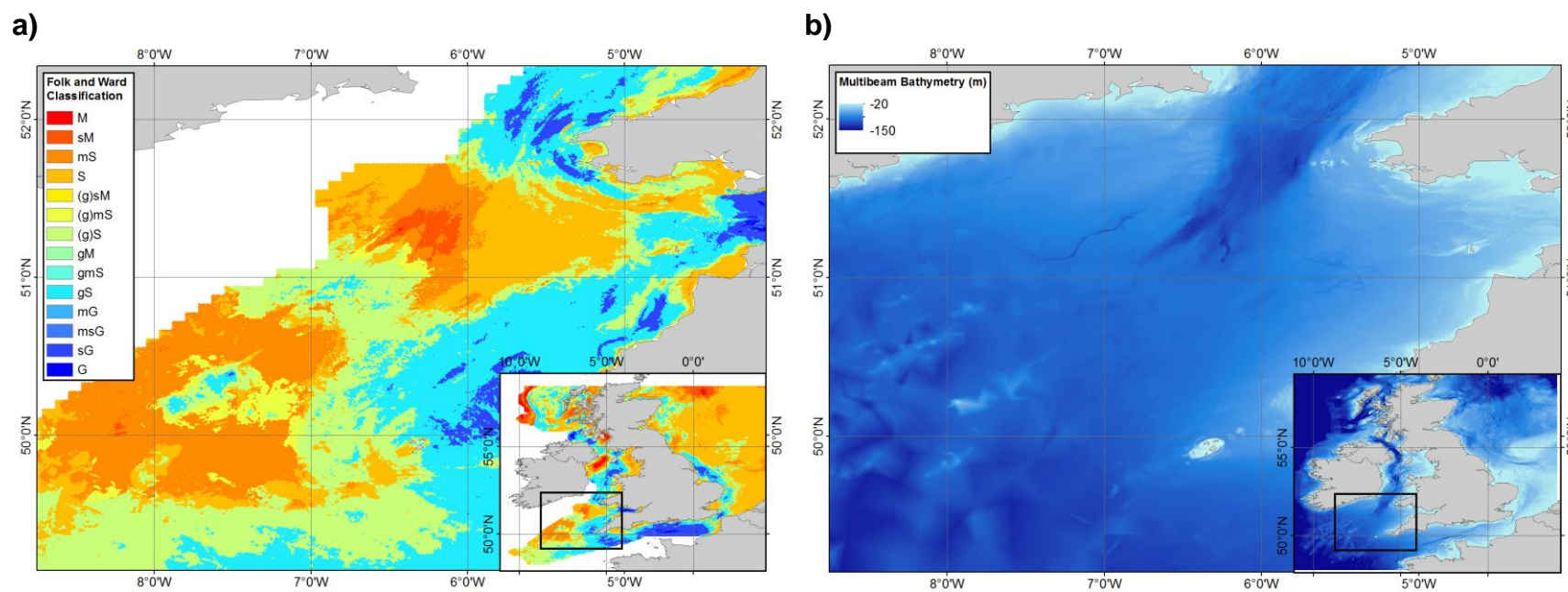
1407 **Online Resource 4** Sidescan of the 4 study sites: (a) Site A, (b) Site G, (c) Site H and (d) Site I. All
 1408 scale bars represent 100 m. The parallel white lines are the nadir and represent lines with no data.
 1409 Note that at Site G, the white vertical band represents an area where no data were collected. The
 1410 presence of repeating backscatter ‘stripes’ at Site G is clear and appear to be matched by
 1411 bathymetric variations suggestive of sedimentary bedforms. Presumed “trawl marks” (seabed scars
 1412 resulting from commercial bottom trawling operations) are particularly notable at Site I, but also
 1413 present at sites A, G and H

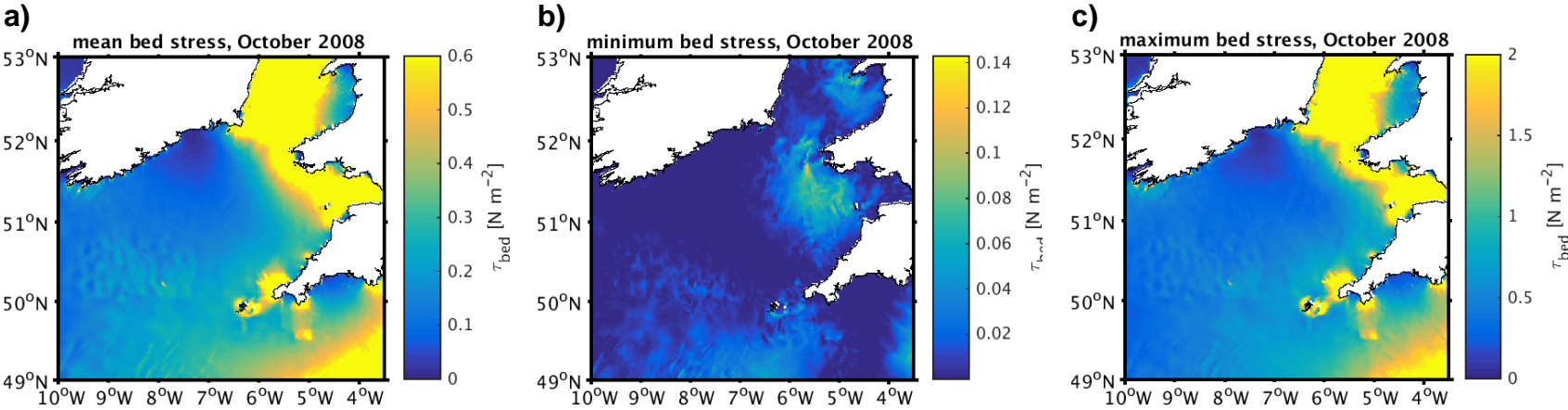
1414

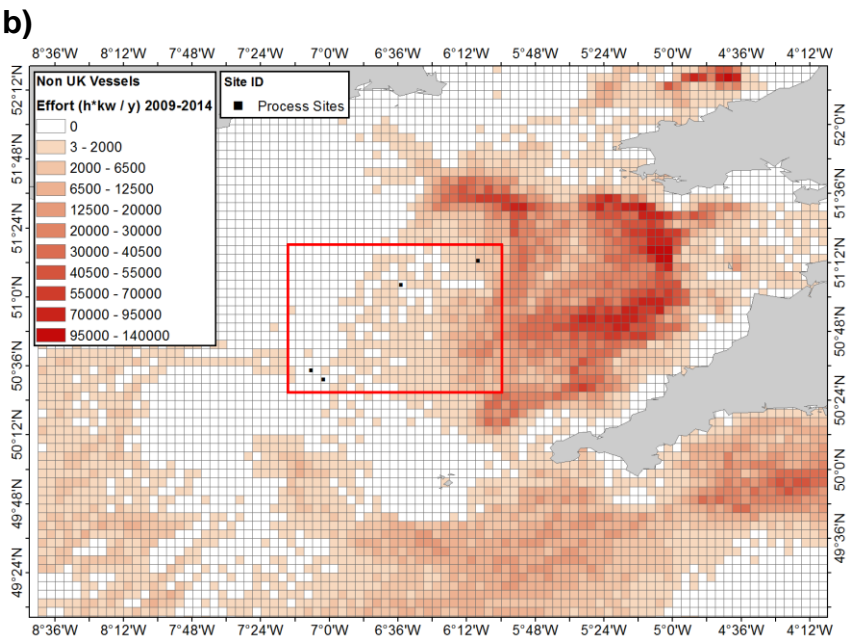
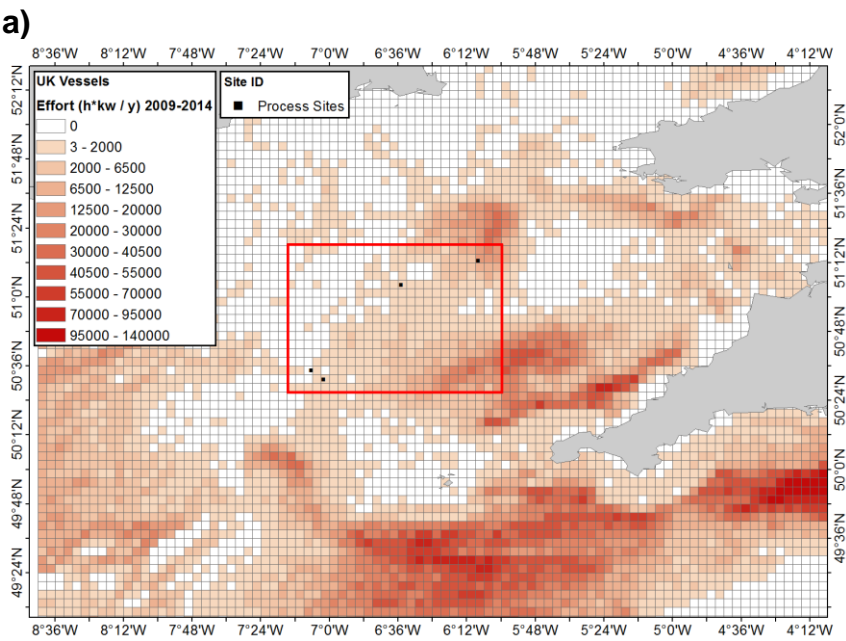
1415 **Online Resource 5** Mean Nutrient Fluxes (mmol.m⁻².d⁻¹) averaged over all seasons: Boxes
 1416 represent mean and SE, with max and min whiskers

1417 **Online Resource 6** Example of density dominant fauna across sites G, H and I. Taxa were
 1418 determined to the lowest taxonomic level whenever possible (otherwise a morphotype was

1419 assigned). Arthropoda (a) *Nephrops norvegicus* and (d) *Goneplax rhomboides*; Echinodermata
1420 Asteroidea (b) *Astropecten irregularis*, (f) *Luidia sarsii*; and, Cnidaria (c) *Cnidaria spp.* type 01, (f)
1421 *Bolocera spp.* type 01
1422 **Online Resource 7** Site specific species abundance
1423 **Online Resource 8** AMBI scores for the four process sites. (Borja et al, 2000)
1424







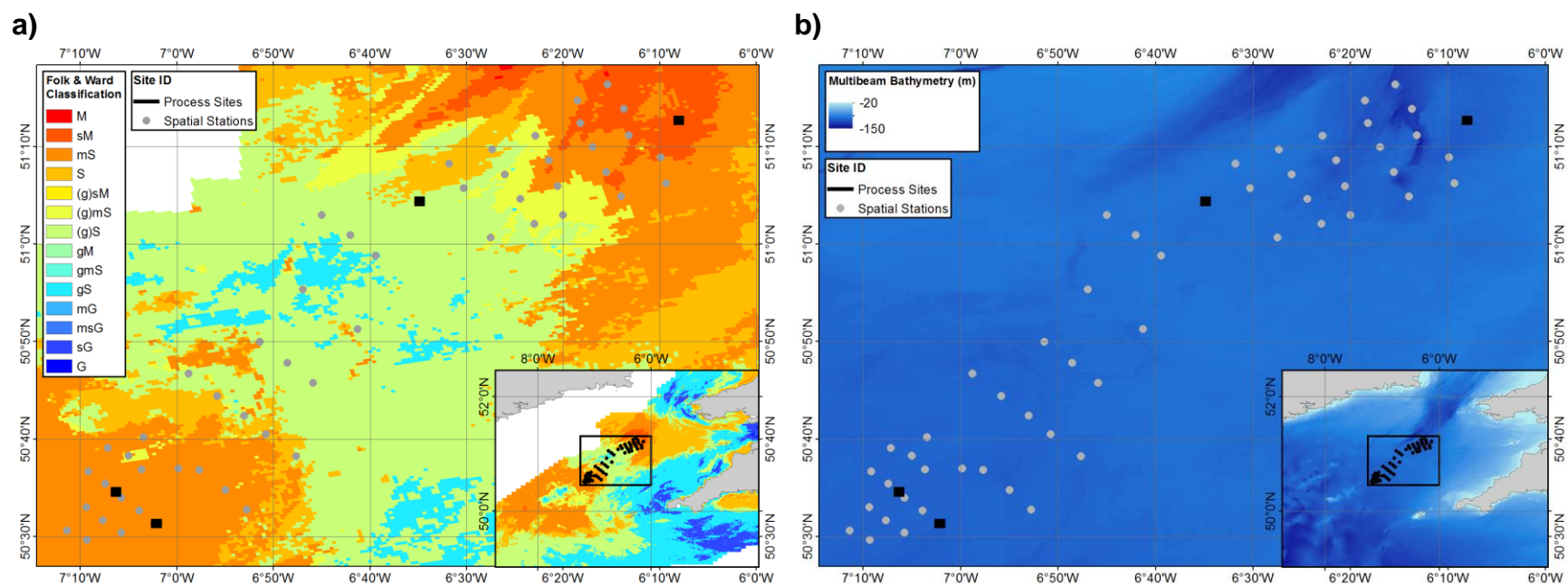
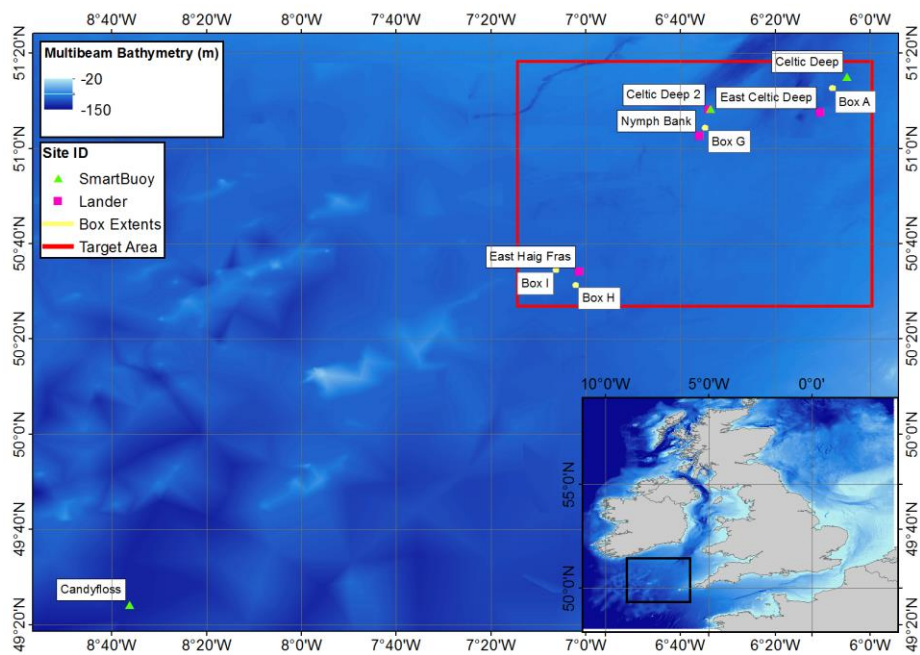
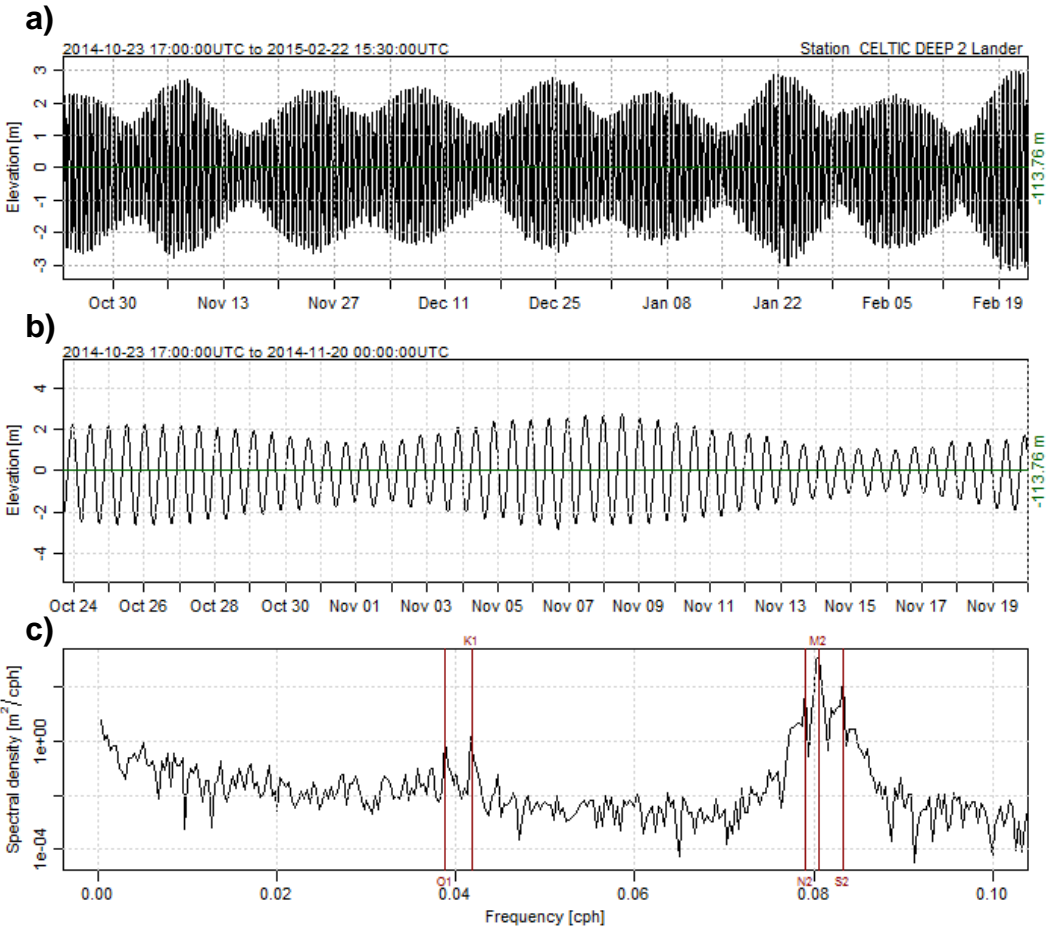


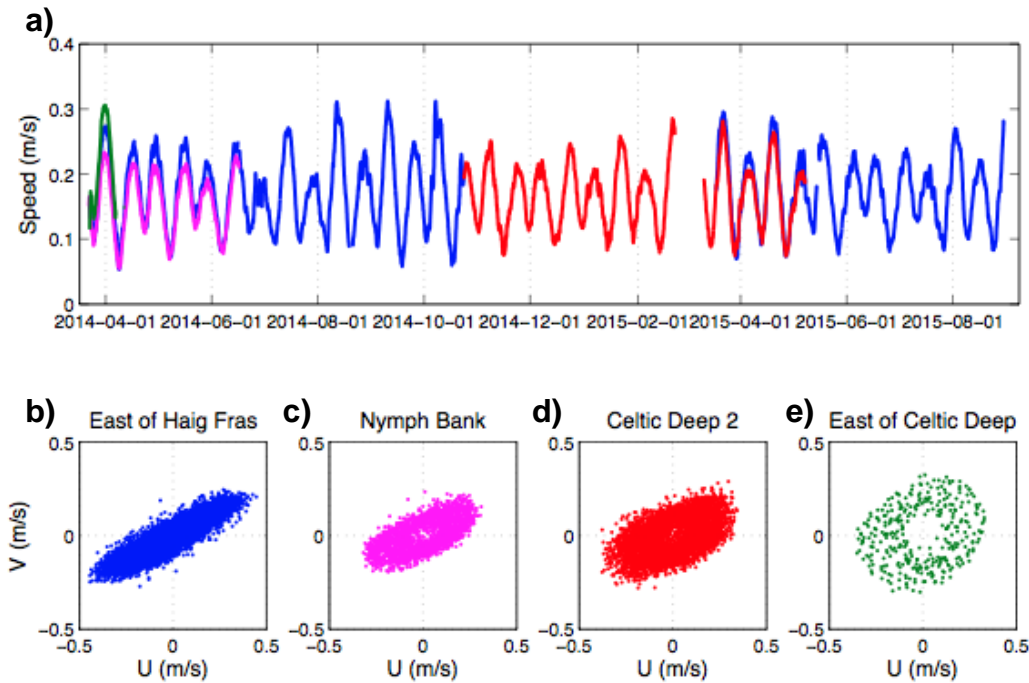
Figure 5



1)



2)



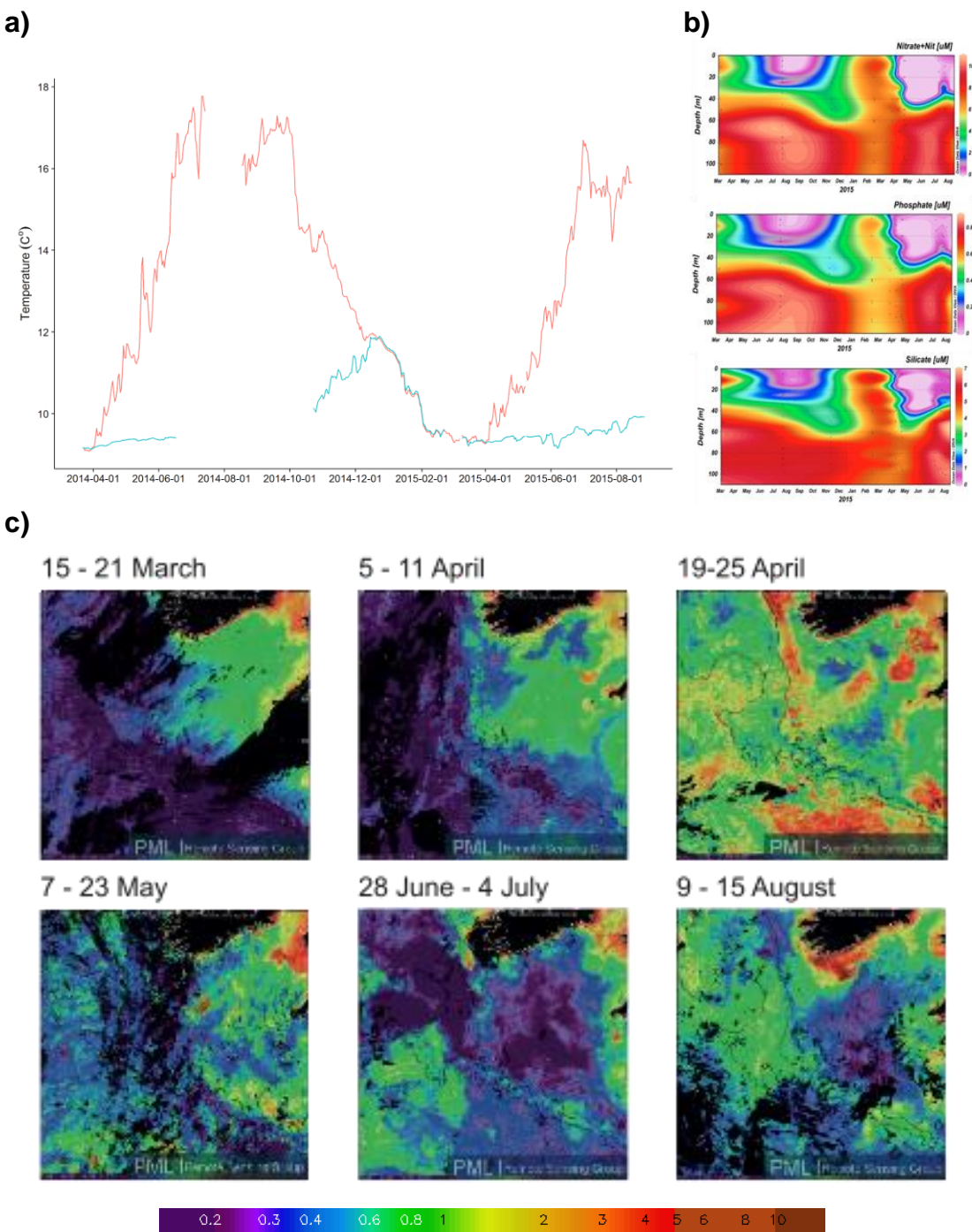
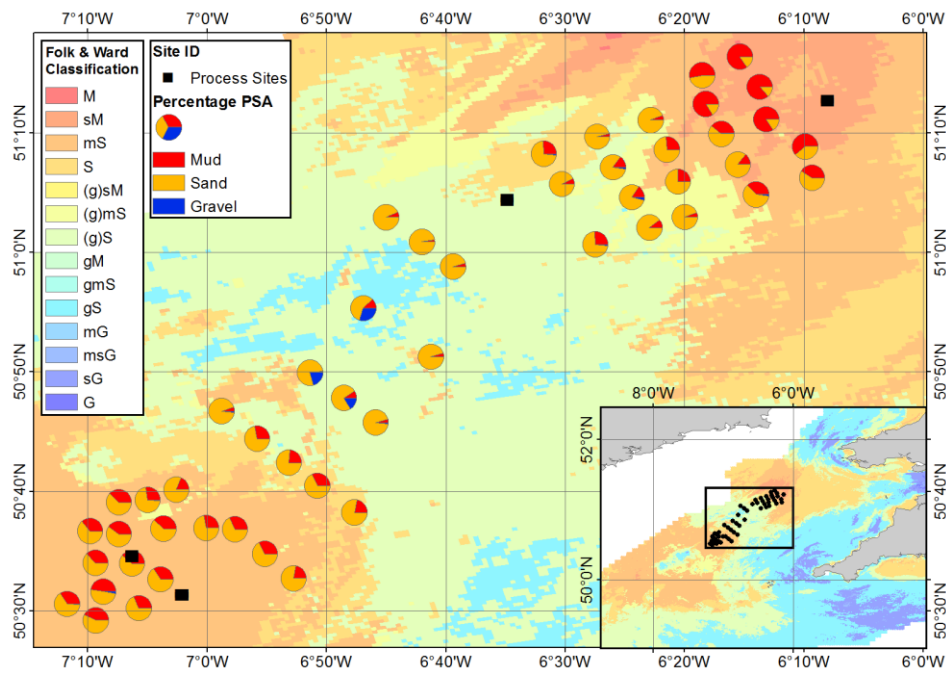
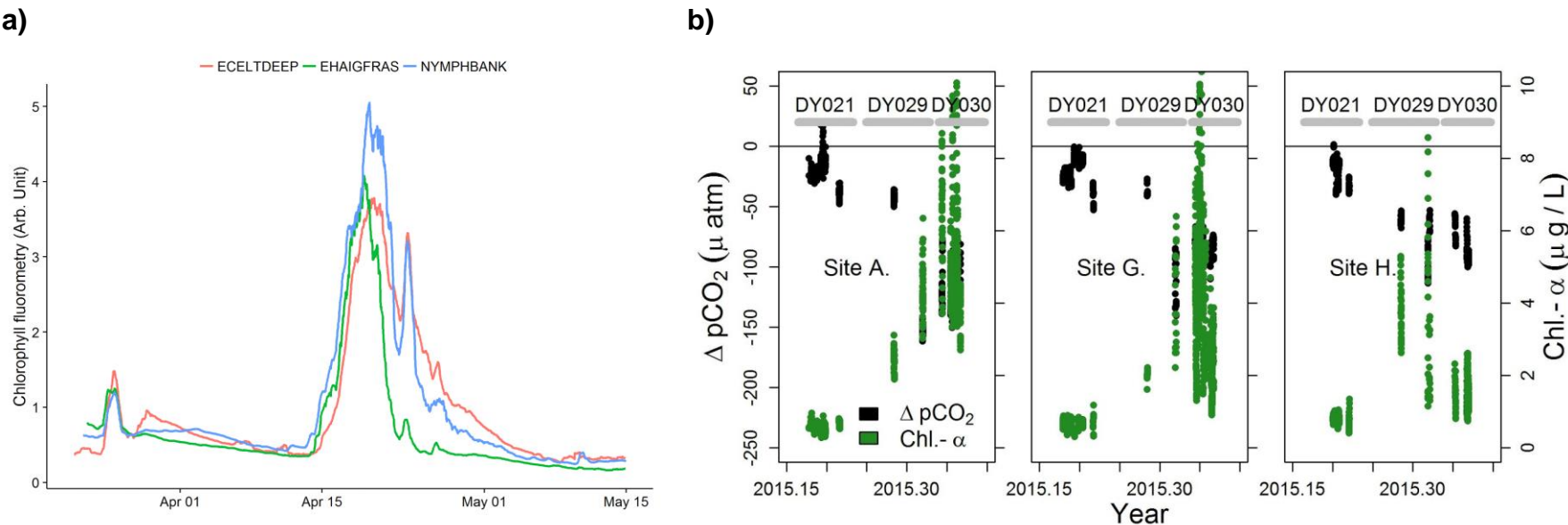
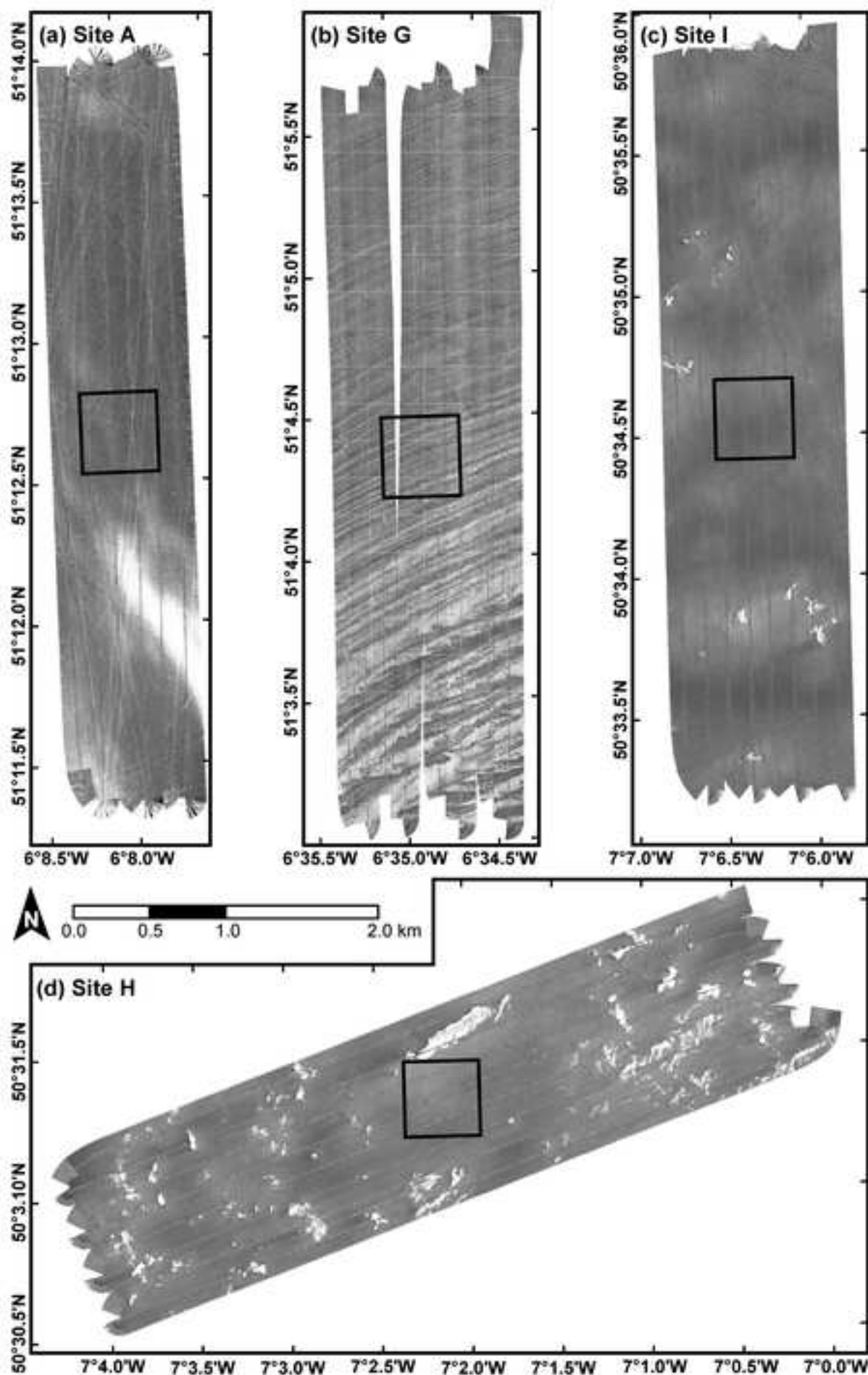
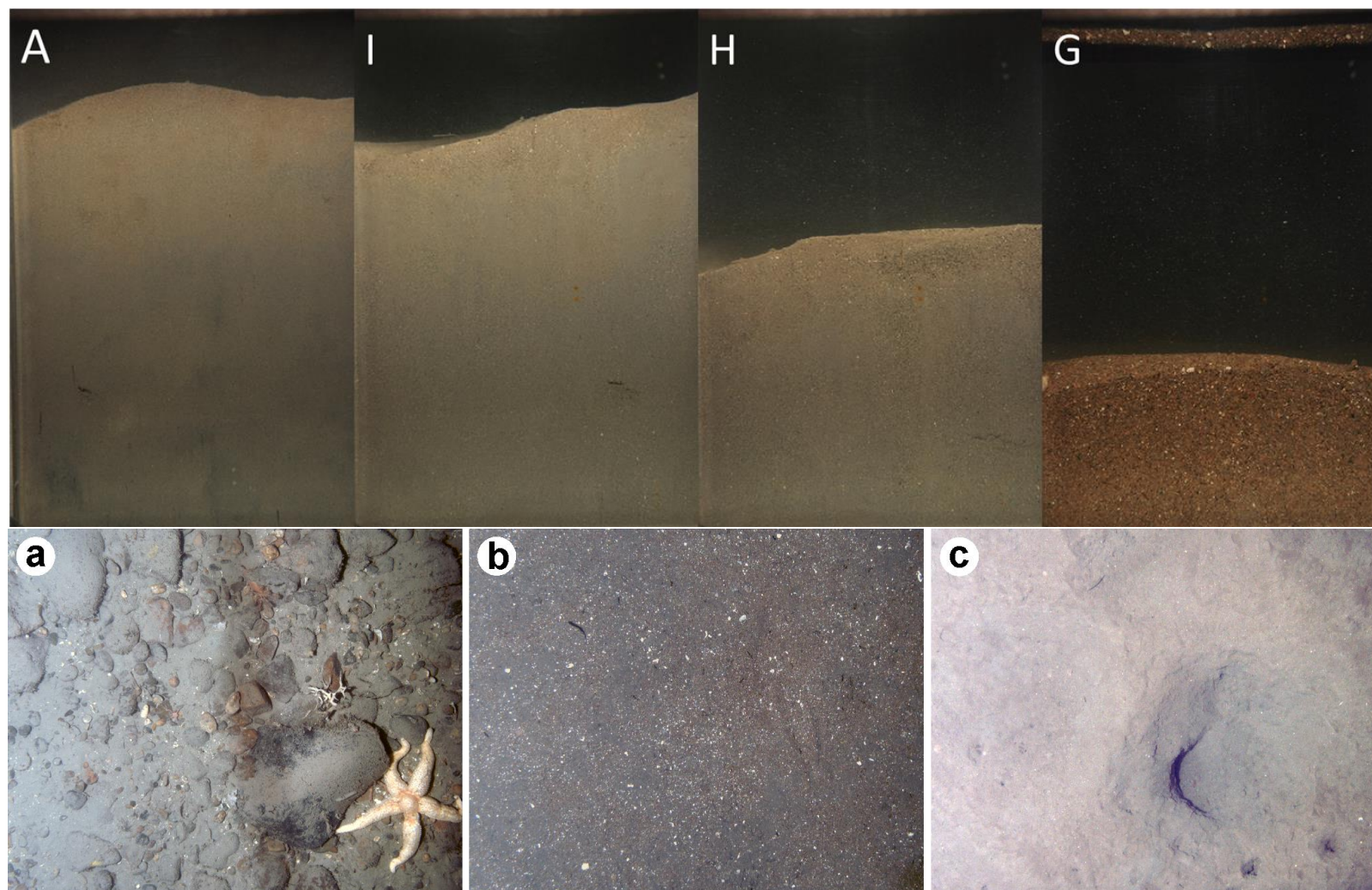


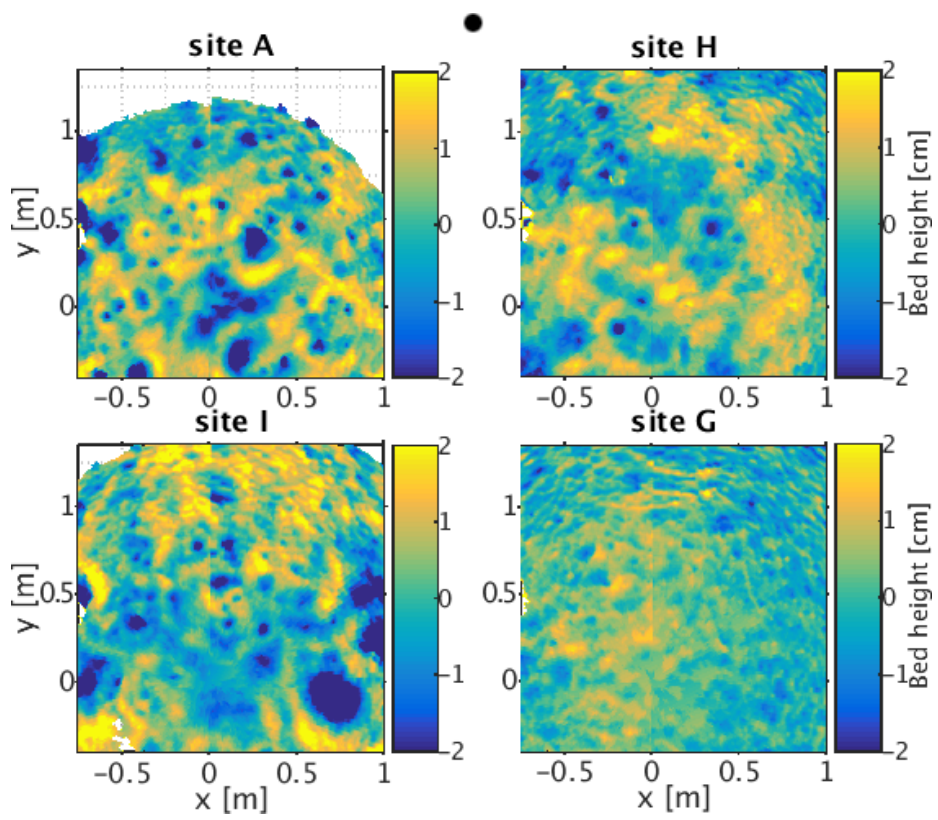
Figure 8



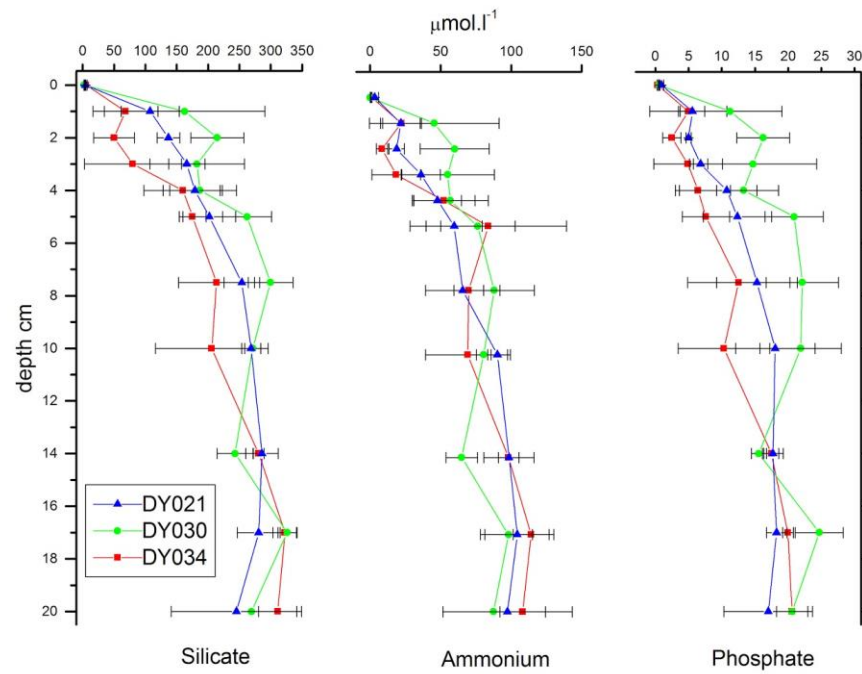




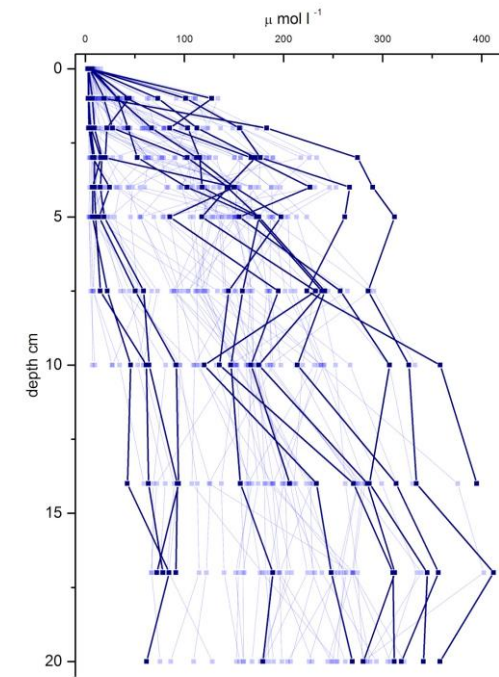




a)



b)



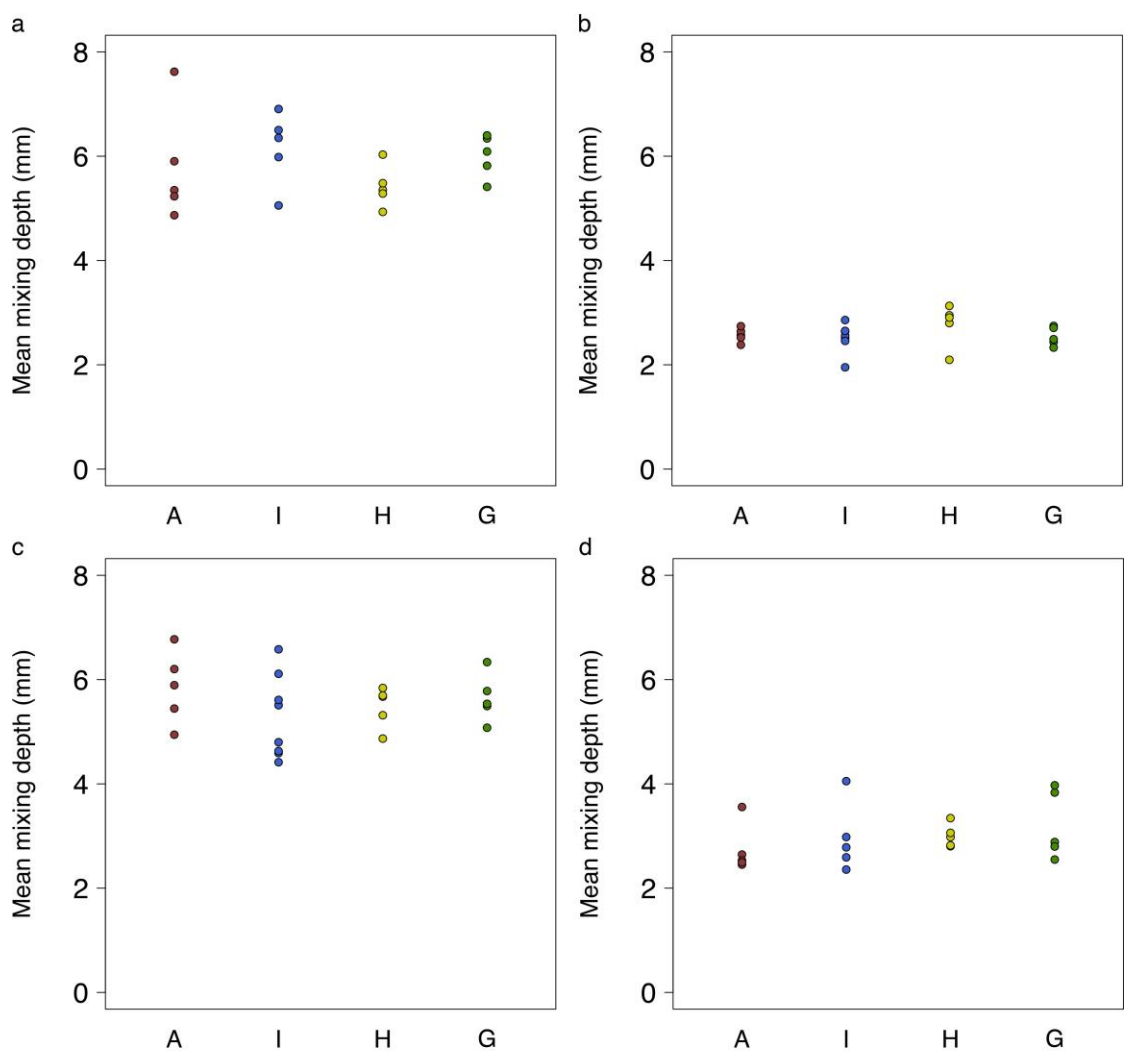
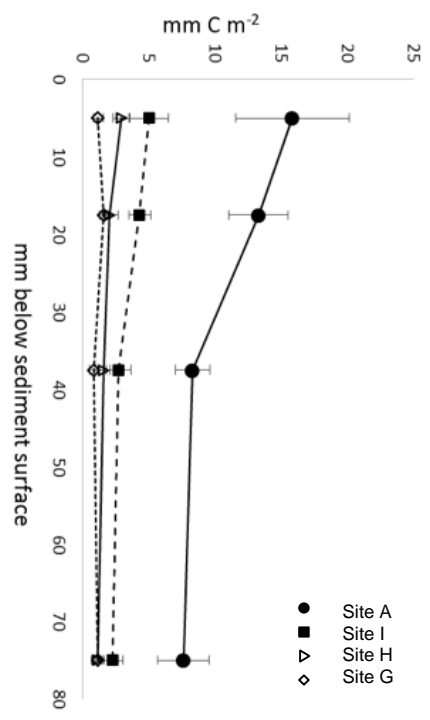
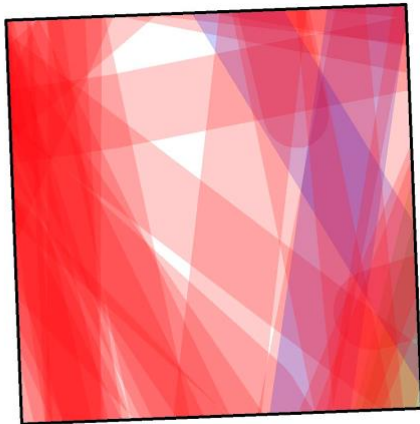


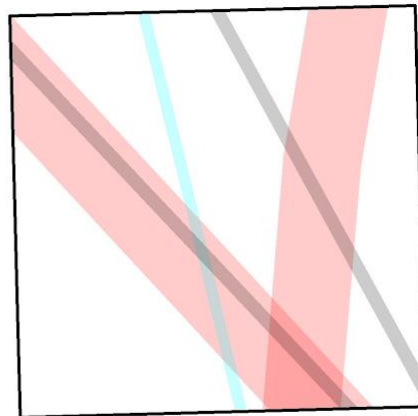
Figure 15



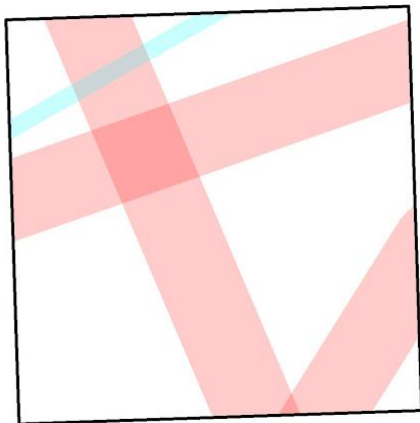
A: Mud



H: Muddy sand



G: Sand



I: Sandy mud

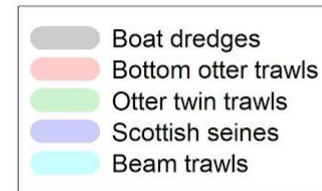
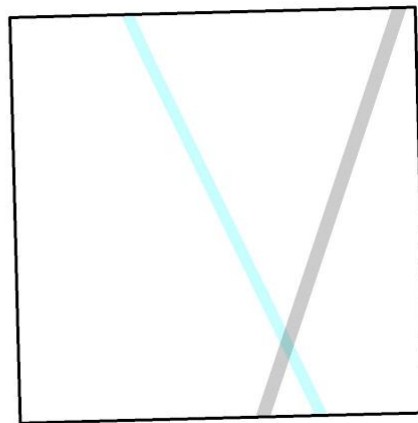


Table 1: Percentage coverage of Folk Textural Classification categories for the target area in Figure 1a and Figure_4a, based on Folk textural classification predictions of surficial sediment type, highlighting those sediment types which comprise >10% of the total (Stephens, 2015; Stephens & Diesing, 2015; *Folk, 1954*)

Folk Classification	Percentage Coverage of Celtic Sea (%)	Percentage Coverage of target area (%)
<i>Mud: M</i>	0.005	0.033
<i>sandy Mud: sM</i>	0.838	3.724
<i>muddy Sand: mS</i>	15.879	23.702
<i>Sand: S</i>	16.358	13.069
<i>(gravelly) muddy Sand: (g)mS</i>	2.601	4.393
<i>(gravelly) Sand: (g)S</i>	24.101	43.079
<i>gravelly muddy Sand: gmS</i>	0.150	0.028
<i>gravelly Sand: gS</i>	31.294	11.952
<i>muddy sandy Gravel: msG</i>	0.165	-
<i>sandy Gravel: sG</i>	8.373	0.020
<i>Gravel: G</i>	0.057	-

Table 2: Sampling and cruise periods, with central points of each 500m x 500m process site box.

Cruise ^a	Start Date	End Date	Description	
DY008	18 March 2014	13 April 2014	Pre-bloom, site identification and ground truthing	
DY021	01 March 2015	26 March 2015	Pre-bloom, Spatial Survey	
DY030	04 May 2015	25 May 2015	Bloom	
DY034	06 August 2015	02 September 2015	Post-Bloom	
Process Site Name	Benthic A	Benthic I	Benthic H	Benthic G
Central Point Location	51° 12.6754 -6° 8.0277	50° 34.5557 -7° 6.3161	50° 31.3329 7° 2.142	51° 4.3569 -6° 34.866

^aBenthic sampling cruises which took place aboard the RRS Discovery. Where available cruise reports and data inventories can be found at the following link: http://www.uk-ssb.org/research_cruises/programme.

Table 3: Continuous monitoring Lander data.

Site	Pressure ^a (dBar)	Temperature (°C)	Salinity	Turbidity (FTU)	O ₂ saturation (%)
East of Celtic Deep	104 ± 1.5 (n = 6285) (100 - 107)	9.56 ± 0.2 (n = 6285) (9.22 – 10.46)	35.23 ± 0.01 (n = 3200) (35.1 – 35.27)	9.2 ± 13 (n = 2393) (1.3 – 178.2)	98.4 ± 3.4 (n = 3200) (91.7 – 103.9)
Nymph Bank	110.5 ± 1.5 (n = 4173) (107.6 – 113.5)	9.32 ± 0.09 (n = 4173) (9.12 – 9.46)	35.2 ± 0.0 (n = 4173) (35.13 – 35.24)	4.3 ± 8.4 (n = 6167) (0.6 – 89.8)	97 ± 5.3 (n = 4173) (87 – 104)
East of Haig Fras	107.5 ± 1.3 (n = 23702) (104 – 111.7)	10.13 ± 0.61 (n = 23704) (9.15 – 11.81)	35.26 ± 0.05 (n = 12926) (34.86 – 35.36)	2.5 ± 4.6 (n = 24257) (0.4 – 78)	91 ± 7.0 (n = 10996) (82 – 103)
Celtic Deep 2 Lander	100.6 ± 109.6 (n = 13975) (94.6 – 107.9)	10.4 ± 0.8 (n = 13975) (9.1 – 11.9)	35.14 ± 0.16 (n = 6407) (34.67 – 35.36)	2.3 ± 2.2 (n = 14953) (0.5 – 65.5)	83 ± 12.9 (n = 6098) (63 – 106)

^aPressure at seabed

Table 4: Sediment characterization and structural parameters for the four process study sites.

Site	Median Grain Size (d ₅₀ , µm)	Mean Grain Size ^a	Sorting ^a	Skewness ^a	Kurtosis ^a	% Fines ^b	Folk Class ^c	Dry Bulk Density (kgm ⁻³)	Porosity	Specific Permeability ^d (x10 ⁻¹⁴ m ²)
Benthic A	57.30 ± 25.70 (n = 20) (15.69-145.66)	37.64 ± 18.5 (n = 20) (15.71-108.24)	4.78 ± 0.52 (n = 20) (4.13-6.18)	-0.45 ± 0.10 (n = 20) (-0.53--0.08)	1.00±0.13 (n = 20) (0.68-1.39)	53.65 ± 10.76 (n = 20) (24.04-72.89)	Sandy Mud	835.57 ± 142.27 (n=12) (735.45-1041.11)	0.68 ± 0.05 (n=12) (0.61-0.72)	2.16 ± 2.10 (n=12) (0.59-5.25)
Benthic I	121.51 ± 30.33 (n = 20) (51.88-197.52)	88.62 ± 35.13 (n = 20) (33.63-177.69)	4.56 ± 0.83 (n = 20) (3.63-6.37)	-0.40±0.10 (n = 20) (-0.61--0.25)	1.36 ± 0.22 (n = 20) (0.94-1.69)	28.36 ± 8.01 (n = 20) (17.10-53.16)	Muddy Sand	1119.43 ± 137.98 (n=12) (983.03-1247.11)	0.58 ± 0.05 (n=12) (0.53-0.63)	15.4 ± 6.53 (n=12) (9.12-23.3)
Benthic H	177.63 ± 97.96 (n = 22) (79.48-518.22)	145.67 ± 104.33 (n = 22) (37.05-509.77)	4.19 ± 1.16 (n = 22) (1.88-6.43)	-0.37±0.11 (n = 22) (-0.63--0.11)	1.41 ± 0.26 (n = 22) (0.82-1.87)	21.92 ± 8.93 (n = 22) (4.88-43.82)	Muddy Sand	1182.19 ± 61.09 (n=12) (1121.40-1261.08)	0.55 ± 0.02 (n=12) (0.52-0.58)	57.4 ± 46.6 (n=12) (25.6-125.4)
Benthic G	458.83 ± 175.14 (n = 20) (48.26-730.33)	445.95 ± 188.75 (n = 20) (29.35-715.82)	3.05 ± 1.9 (n = 20) (1.65-9.58)	-0.30±0.24 (n = 20) (-0.66-0.36)	2.17 ± 0.89 (n = 20) (0.48-3.20)	13.05 ± 16.69 (n = 20) (1.98-56.28)	Sand	1493.07 ± 178.36 (n=12) (1299.84-1714.14)	0.44 ± 0.07 (n=12) (0.35-0.51)	693.6 ± 180.1 (n=12) (491.7-857.4)

^aFolk and Ward (1957) geometric (modified) graphical (µm) measures. ^bFines <63µm. ^cFolk (1954) textural class. ^dEngelund, 1953

Values are means of all samples collected at the sites, ± standard deviations (min-max ranges in brackets) and represent bulk samples 0-5cm in depth, referred to as 'surface' samples.

Table 5: Biogeochemical Parameters

	Bulk Properties ^a												
Site	Organic Carbon (%) ^d	Organic Nitrogen (%) ^d	Oxygen Penetration Depth (cm) ^e	Total Oxygen Consumption (mmol ⁻² d ⁻¹) ^f	Chlorophyll (□g.g ⁻¹) ^g	Zone of Mixing (cm) ^h	Surface Roughness (cm) ^h						
Benthic A	1.12 ± 0.13 (0.98 - 1.34)	0.13 ± 0.02 (0.10 - 0.17)	0.875 ± 0.54 (0.3 - 1.6)	-7.62 ± 2.78 (n = 44) (-15.54 - -3.04)	1.43 ± 0.60 (0.68 - 2.1)	6.28 ± 0.98 (3.69 - 7.30)	1.85 ± 0.79 (0.92 - 3.20)						
Benthic I	0.58 ± 0.15 (0.39 - 0.84)	0.09 ± 0.03 (0.04 - 0.14)	0.725 ± 0.60 (0.20 - 1.50)	-9.93 ± 4.96 (n = 39) (-22.16 - -3.17)	0.47 ± 0.17 (0.22 - 0.6)	5.23 ± 1.54 (3.32 - 8.01)	1.83 ± 0.53 (1.20 - 3.30)						
Benthic H	0.42 ± 0.12 (0.31 - 0.65)	0.07 ± 0.02 (0.04 - 0.11)	0.875 ± 0.49 (0.3 - 1.5)	-9.32 ± 3.80 (n = 41) (-17.19 - -2.39)	0.42 ± 0.18 (0.3 - 0.64)	4.55 ± 1.27 (3.05 - 7.47)	1.82 ± 0.35 (1.25 - 2.46)						
Benthic G	0.22 ± 0.18 (0.11 - 0.49)	0.06 ± 0.04 (0.02 - 0.12)	2.08 ± 2.00 (0.5 - 5)	-5.17 ± 3.50 (n = 35) (-13.43 - 0.66)	0.33 ± 0.26 (0.08 - 0.62)	n/a	1.50 ± 0.89 (0.61 - 4.50)						
	Porewater Concentrations (□M) ^b							Diffusive Fluxes (mmol.m ⁻² .d ⁻¹) ^c					
Site	Nitrite (NO ₂ ⁻)	TOxN (NO ₂ ⁻ + NO ₃ ⁻)	Ammonium (NH ₄ ⁺)	Silicate (SiO ₄ ⁻)	Phosphate (PO ₄ ³⁻)	Iron (Fe) ⁱ	Iron (Fe(II)) ⁱ	Nitrite (NO ₂ ⁻)	TOxN (NO ₂ ⁻ + NO ₃ ⁻)	Ammonium (NH ₄ ⁺)	Silicate (SiO ₄ ⁻)	Phosphate (PO ₄ ³⁻)	Iron (Fe(II)) ⁱ x10 ⁻³
Benthic A	0.46 ± 0.37 (0.07 - 8.27)	4.45 ± 3.60 (0.33 - 12.8)	38.3 ± 30.1 (0.29 - 144)	134 ± 83.8 (5.72 - 339)	7.61 ± 5.94 (0.93 - 28.4)	4 ± 6 (0.1 - 10)	3 ± 5 (0.08 - 9)	0.013 ± 0.031 (-0.017 - 0.098)	0.019 ± 0.174 (-0.212 - 0.499)	0.021 ± 0.156 (-0.286 - 0.483)	1.212 ± 0.679 (0.206 - 3.741)	-0.018 ± 0.024 (-0.063 - 0.028)	14.4 ± 19.7 (-0.01 - 54.4)
Benthic I	0.58 ± 0.75 (0.10 - 3.14)	4.26 ± 2.97 (0.20 - 17.9)	38.3 ± 30.9 (0.23 - 145)	146 ± 88.5 (3.14 - 358)	7.55 ± 5.98 (0.25 - 29.0)	7 ± 7 (3 - 15)	12 ± 15 (3 - 29)	0.012 ± 0.021 (-0.007 - 0.064)	0.125 ± 0.267 (-0.286 - 0.644)	-0.003 ± 0.145 (-0.077 to 0.380)	0.646 ± 0.430 (-0.049 - 1.550)	0.001 ± 0.029 (-0.080 - 0.054)	8.30 ± 10.3 (0.23 - 32.8)
Benthic H	0.78 ± 1.52 (0.09 - 1.74)	4.63 ± 4.00 (0.08 - 9.2)	38.6 ± 27.8 (0.29 - 107)	145 ± 82.0 (5.39 - 347)	7.68 ± 5.70 (0.86 - 25.7)	0.5 ± 0.7 (0.11 - 1.3)	0.5 ± 0.7 (0.1 - 1.3)	0.011 ± 0.038 (-0.035 - 0.132)	0.082 ± 0.286 (-0.586 - 0.649)	0.049 ± 0.191 (-0.215 - 0.699)	0.702 ± 0.612 (-0.287 - 2.016)	0.004 ± 0.028 (-0.073 - 0.086)	2.7 ± 5.47 (0.06 - 16.8)
Benthic G	0.74 ± 1.19 (0.09 - 2.87)	4.47 ± 3.56 (0.19 - 16.6)	40.3 ± 30.3 (0.55 - 114)	153 ± 88.1 (5.93 - 368)	7.47 ± 5.55 (1.08 - 21.2)	n/a	n/a	0.024 ± 0.030 (-0.008 - 0.105)	0.059 ± 0.133 (-0.131 - 0.599)	0.044 ± 0.023 (-0.257 - 0.319)	0.531 ± 0.474 (-0.007 - 2.255)	0.009 ± 0.035 (-0.085 - 0.070)	n/a

Values are means of all samples collected at the sites, ± standard deviations (min-max ranges in brackets) and represent: ^asamples 0-5cm in depth, referred to as 'surface' samples; ^bSamples collected seasonally at the sites from triplicate porewater profiles (n=9) representing 0- 10cm depth; ^cfluxes calculated at each site (n = 5-11) ± standard deviations (min-max ranges in brackets). ^dKirsten (1979); ^eMeasured immediately from 20cm diameter cores, sub-sampled from NIOZ box cores; Cai and Sayles (1996); ^fGlud (2008), Hicks et al. (in prep), Smith et al. (in prep); ^gMeasured using Spectrophotometry (for DY008, HMSO (1980)) or Fluorescence (Tett, 1987); ^hDerived from SPI, Solan et al (2004); ⁱIron values are for surface (0-2 cm) only: not measured at Benthic G; ^jHomocly et al., 2012.

Table 6: Biological Parameters

	Epifauna			Macro-infauna (>1mm)			Meifauna			Microbes	Bioturbation Metrics (mm)				
Site	Abundanc e (ind.m ⁻²)	Blotted wet weight biomass (g.m ⁻²)	Diversity (species)	Abundanc e (ind.m ⁻²)	Blotted wet weight biomass (g.m ⁻²)	Diversity (species)	Abundanc e (k = 1000x ind.m ⁻²)	Calculated wet weight biomass (g.m ⁻²) ^a	Diversity (phyla)	% archaeal 16S rRNA genes	BPc	f-SPI _{Lmax}	f-SPI _{Lmax}	f-SPI _{Lmed}	SBR
Benthic A	0.88 ± 0.56	2.29 ± 1.65	54	957 ± 603	35.7 ± 82.7	21.2 ± 4.8	806k ± 281k	1.13 ± 0.35	5.7 ± 1.3	29.7 ± 16.5	36.70 ± 22.53	13.12 ± 6.67	4.24 ± 1.70	4.11 ± 1.62	16.27 ± 11.27
Benthic I	0.9 ± 1.02	0.75 ± 0.23	78	1190 ± 816	10.2 ± 21.4	31.2 ± 10.6	556k ± 242k	1.14 ± 0.48	6.4 ± 2.0	35.8 ± 15.9	19.11 ± 13.14	11.62 ± 4.84	4.35 ± 1.56	4.22 ± 1.49	15.10 ± 7.85
Benthic H	0.8 ± 0.7	0.57 ± 0.34	128	1130 ± 521	14.0 ± 1.4	37.6 ± 8.1	596k ± 222k	0.73 ± 0.39	4.8 ± 1.2	38.3 ± 20.9	30.31 ± 20.33	15.09 ± 12.32	4.17 ± 1.32	4.08 ± 1.33	14.14 ± 8.80
Benthic G	1.57 ± 1.61	1.82 ± 0.88	115	483 ± 291	16.0 ± 23.0	21.1 ± 9.1	560k ± 178k	0.68 ± 0.17	5.9 ± 2.0	22.2 ± 14.2	25.01 ± 17.70	10.03 ± 4.52	4.37 ± 1.64	4.30 ± 1.61	14.69 ± 9.37
Seabed Photography															
Site	Megafauna		Demersal Fish		Invertebrates										
	Density (ind.m ²)	Biomass (gm ⁻²)	Density (ind.m ²)	Biomass (gm ⁻²)	Density (ind.m ²)	Biomass (gm ⁻²)									
Benthic I	0.53 (0.48-0.59)	6.43 (6.26-6.61)	0.09 (0.07-0.11)	5.21 (5.05-5.41)	0.40 (0.35-0.44)	1.04 (1.03-1.05)									
Benthic H	0.59 (0.53-0.65)	14.5 (13.6-15.5)	0.06 (0.05-0.07)	8.75 (8.05-9.50)	0.48 (0.43-0.54)	2.60 (2.52-2.68)									
Benthic G	0.57 (0.51-0.63)	4.77 (4.65-4.90)	0.08 (0.07-0.10)	2.54 (2.43-2.64)	0.44 (0.40-0.49)	2.45 (2.37-2.53)									

Discussion of specific species abundance can be found in Online Reference 7.
^aBased on nematodes



[Click here to access/download](#)

Electronic Supplementary Material
Online Resource1.docx





[Click here to access/download](#)

Electronic Supplementary Material
Online Resource2.docx





[Click here to access/download](#)

Electronic Supplementary Material
OnlineResource3.tif





[Click here to access/download](#)

Electronic Supplementary Material
OnlineResource4.tif





[Click here to access/download](#)

Electronic Supplementary Material
OnlineResource5.docx





[Click here to access/download](#)


Electronic Supplementary Material
OnlineResource6.tif





[Click here to access/download](#)

Electronic Supplementary Material
OnlineResource7.pdf





[Click here to access/download](#)

Electronic Supplementary Material
OnlineResource8.docx

